

# **Chapter-1**

## **Introduction and Literature Review**



## **1.1 Need for high Energy Storage device in Medical applications**

The world has witnessed significant growth in electronics, micro and nano-fabrication, and wireless technology, which have greatly enhanced the quality and efficacy of healthcare and life-science research [1-5]. Biomedical devices, whether portable or implantable, have long been used to improve healthcare by supporting the restoration of biological functionality. These devices are utilized for prognosis, diagnosis, assistance, treatment, and other health-related needs. Most biomedical devices require a steady and sufficient power source to function properly. The reliability of medical equipment is very crucial. If a power outage occurs in a biomedical device or healthcare facility centre, shutting down electronic instruments and systems can put many lives at risk. When a power disruption occurs, although most systems are ready to recover and resupply power, sometimes it can take up to a minute to connect to the generator or a new emergency power backup, a time that in the hospital environment is precious and can mean the difference between life and death. Given how delicate and dangerous it can be for a hospital to be left without a power supply, the need for UPS (uninterruptible power supply) devices becomes a compulsion because it can save lives by preventing vital medical equipment like ventilators and other life support systems from shutting down. Batteries are the heart and the most essential element of a UPS system. Without a powerful battery, the device does not work. UPS batteries provide a constant power supply for a certain amount of time, enabling crucial systems to function normally until the primary power source is restored.

Health professionals in rural clinics face many challenges on a daily basis [6,7]. Not only a lack of qualified medical staff, equipment and medicine can become a major obstacle in providing crucial basic health services for the rural population, also lacking or unreliable energy supply can be a severe problem. Recent advancements in energy systems have made

it feasible to deliver basic healthcare services, including vaccinations, to rural places at a reasonable cost.

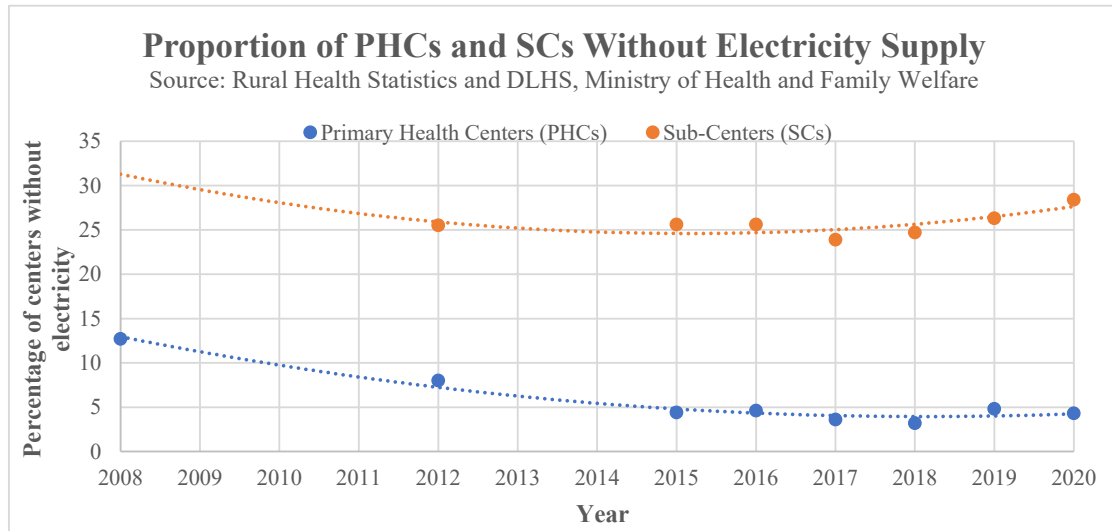


**Figure 1.1-** Proportion of PHCs and SCs in India without electricity supply

The Rural Health Statistics for the year 2018-19 highlights an important data point regarding the availability of electricity and power backup at rural Health and Wellness Centres (upgraded Sub-Centres). Out of a total of 7,821 HWCs located in rural India, merely 3,496, representing 45%, are equipped with a power backup facility [8].



**Figure 1.2-** Electrification option for rural health clinic (Figure is taken from open access internet source)

Hybrid Renewable Energy Sources (HRES) microsystems, like microgrids incorporated with solar panels and battery, is identified to ensure higher and more reliable energy access in rural healthcare centres.

## 1.2 Types of devices used in Biomedical applications

In contrast to pharmaceuticals or biologics, medical devices accomplish their goals through physical, structural, or mechanical action rather than chemical or metabolic action within or on the body. A medical device can be any instrument, apparatus, machine, tool, implant, in vitro reagent, or similar article intended to diagnose, prevent, mitigate, treat, or cure disease or other conditions [9].

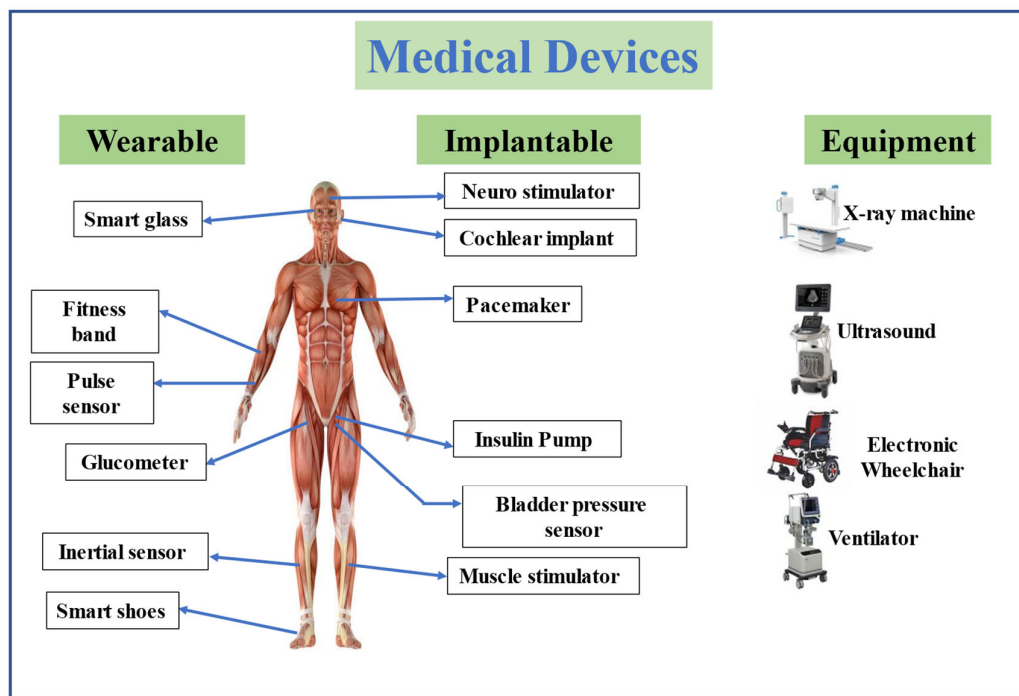


*Figure 1.3- Different types of Biomedical equipment*

There are two main ways in which biomedical equipment is utilized to enhance the quality of life of humans. The first is where devices and power sources are external to the part of the body where the particular equipment functions, and the second is where the device can

be implanted at the site of action, and the battery can be either external or implanted in a different but convenient location.

### **1.2.1 Medical application using External devices**

Biomedical equipment is the devices that employ one or more electrical, electronic, or mechanical methods for health care prevention, diagnosis, treatment, or rehabilitation [10].

- **Left Ventricular Assist Devices:** Patients awaiting heart transplants or those with seriously damaged hearts can benefit from LVADs, which are pumping devices affixed directly to the heart. The power needs are too high to fully meet by the implanted secondary batteries. Power is sent to the gadget through the skin utilizing a battery pack worn by the patient.
- **Dynamic Prostheses:** Dynamic prostheses are a type of prosthetic device that can mimic the body's natural movements or provide more dynamic movement and function.
- **Portable Medical Devices:** Portable medical devices have revolutionized how people monitor and determine their health and well-being. From digital stethoscopes to pocket-sized ECGs and portable ultrasounds, the diagnostics potential one can carry in the bag is amazing these days [11].
- **Motorized Wheelchairs:** The electric propulsion system of the economical wheelchair prevents the necessity for manual pushing, allowing effortless movement and reducing user fatigue. The range of power wheelchairs can be increased using wet, rather than gel, batteries and can be over 50 km [12].
- **Life-Support System:** Life-support systems provide all or some elements essential for maintaining physical well-being, for example, oxygen, nutrients, water, disposal of body wastes, and control of temperature and pressure.

## 1.2.2 Implantable Medical Devices

Medical implants [13-16] are devices that are either permanently or temporarily inserted into the body to monitor physiological activity, assist the functionality of particular organs or tissues, or administer medication. Some well-known implantable devices are as follows:

- **Cardiac Pacemakers:** In 1960, the first cardiac pacemaker was introduced to treat bradycardia. The first Li-powered pacemaker was implanted in 1972, and the half a million pacemakers that are presently implanted each year nearly all employ Li/I2-PVP (Poly 2-vinyl pyridine) primary batteries. Congestive heart failure is a leading cause of death that can be treated by biventricular pacing in both the left and right ventricles.
- **Implantable Cardiac Defibrillators:** If left untreated, tachycardia, a medical disorder where the heart beats excessively quickly, can lead to ventricular fibrillation and even death. The first implantable cardiac device (ICD) came into existence in 1980 and employed a Li/V2O5 battery to power an electrode that was sutured onto the heart to detect and halt fibrillation. These days, ICDs serve as pacemakers and treat tachycardia before fibrillation occurs.
- **Neurostimulators:** These are devices that resemble pacemakers and are utilized for a variety of functions, such as pain blocking. For paraplegic patients, Functional Neuromuscular Stimulators have been developed to assist them with walking short distances, up to one mile. A walking frame's finger-touch buttons operate a microprocessor that sends stimulation impulses over the skin to cause action potentials in particular peripheral nerves.
- **Cochlear Implants:** These days, many devices are inserted often, from cochlear implants for the very deaf to converters of acoustic impulses to mechanical energy that are appropriate for patients with some residual hearing.

- **Drug Delivery Systems:** The best results from pharmacological therapy come from administering the medication at the appropriate time and location, which allows for the use of smaller dosages. Implantable drug delivery devices with electronic controls, a transcutaneous replenished drug reservoir, an internal catheter for drug administration, a mechanical bellows pump, or a battery can accomplish targeted delivery and dose programming.

### 1.3 Power requirement of Biomedical devices

Biomedical devices have varying power needs depending on the type of equipment and its intended use [17]. The selection of power supplies for medical uses is a task that must be approached with great care to meet safety and reliability standards. Modern switch-mode power supplies are employed in a wide array of medical equipment, including but not limited to MRI, X-ray, CT scanners, blood analysers, patient monitors, ultrasound, robotic surgical devices, hurt-lung machines, diagnostic equipment, and automated pharmaceutical dispensers. Biomedical devices take power in the few  $\mu\text{W}$  to few kW range. **Fig. 1.4** shows a conceptual illustration (scales may vary) of the power needs of different biomedical devices and the energy source that can cater to those needs.

Modern medical equipment requires power supplies that are compact, lightweight, efficient, cost-effective, Restriction of Hazardous Substances (RoHS) compliant, reliable, and super-safe. For this purpose, energy storage devices like batteries and supercapacitors [18-20] and energy harvesting devices like piezoelectric, triboelectric, thermoelectric, bio-generators, etc [21-24]., are utilized as energy sources. Since their development, rechargeable and non-rechargeable Lithium batteries [25] have been the en-route choice for onboard energy supply in medical devices. The **Fig. 1.4** shows that the batteries and

charging methods can serve the power needs of small-scale medical devices like pacemakers, neuro-stimulators, and high-power-consuming ultrasound machines.

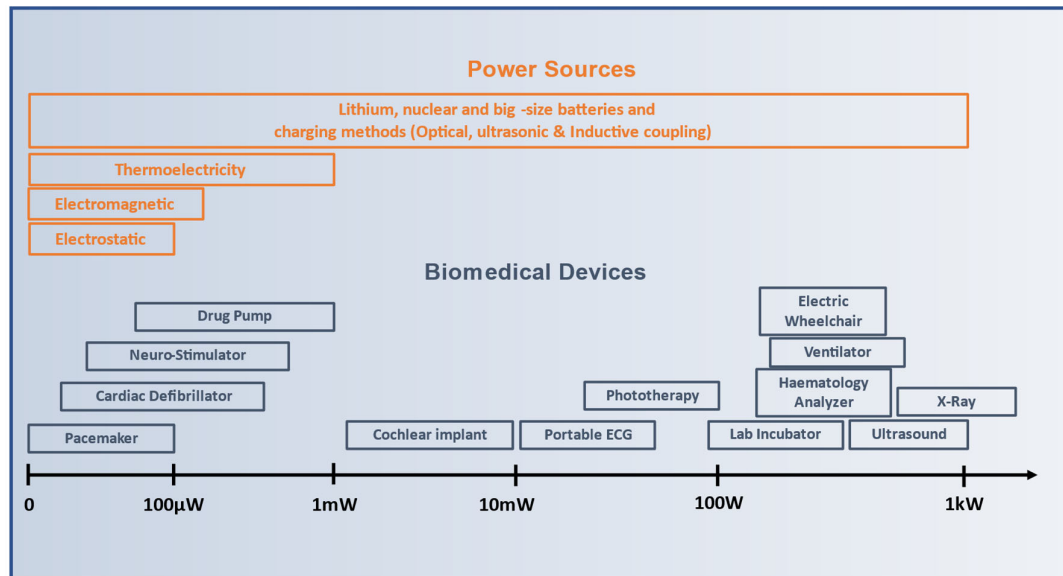


*Figure 1.4- Power ranges of different Biomedical equipment*

## 1.4 Basic Requirements for Biomedical Energy Storage device

Energy storage devices are instrumental in ensuring a consistent and reliable power supply. However, it requires meticulous planning, a clear understanding of your energy needs, and an in-depth assessment before deployment, especially in implantable and wearable medical devices [26-30]. Here are the primary factors that should be considered before deploying an energy storage system for biomedical use:

- **Biocompatibility:** One of the primary criteria is the biocompatibility of the energy storage materials. The assessment of biocompatibility is divided into in-vitro and in-vivo evaluation techniques. Cytotoxicity tests are conducted to assess the toxicity of the implantable medical device or material when it interacts with mammalian cell culture media in an in-vitro setting.

- **Safety and Stability:** While evaluating whether energy storage devices are feasible, safety always comes first. It is imperative that materials used in implantable energy storage devices be biocompatible, free of harmful compounds, and do not cause any immunological or inflammatory reactions at the implant site. Furthermore, the biological environment around an implanted medical device is constantly changing. To safeguard the body, it must be able to carry out its energy storage function in the specified bodily environment for the required duration and without leaking the active components.
- **Miniaturization and Lightweight:** Given that the foreign material is transplanted into particular organs or small areas of subcutaneous tissue, the medical device should be as small and light as feasible to lessen the strain on the surrounding tissue, muscles, and organs.
- **Efficient and Durable:** Different applications showed different impacts on battery degradation mechanisms. Most wearable and biomedical devices are used for long periods and require multiple instances of power supply. Thus, the durability of energy storage devices becomes a critical parameter.
- **Adhesion:** Adhesion properties are critical factors to consider during the fabrication of active devices intended for conformal contact with the human body. Therefore, when these devices are integrated with human skin, it is essential that the adhesion energy exceeds the combined energies associated with substrate bending and skin elasticity.
- **Matching:** Implantable energy storage devices must exhibit particular mechanical characteristics, including Young's modulus, that align with the properties of biological tissue. This compatibility is essential to enable the devices to adjust to the irregularities of the tissue during dynamic deformation without exerting any

mechanical stress. Additionally, it is vital to ensure stable and close contact between surfaces to achieve optimal functionality of the implantable energy storage devices.

## 1.5 Existing Energy Storage Solutions

Currently, batteries are manufactured in various sizes to accommodate a diverse range of applications. The power output varies from watts to several hundred kilowatts, exemplified by the contrast between batteries used for pacemakers and those designed for heavy motor vehicles or power stations. The commonly available secondary batteries, categorized by their electrochemical systems [31-33], can be classified into two primary groups: traditional batteries (lead-acid) and modern batteries (lithium-ion).

### 1.5.1 Primary Lithium-metal batteries for Biomedical Implants

Primary Li-metal batteries are extensively utilized to deliver power levels that vary from microamperes to amperes, catering to the specific requirements of different types of implantable medical devices. Lithium batteries have generally been developed in various configurations, featuring lithium metal anodes paired with a range of cathode systems.

- **Lithium/Iodine (Li/I<sub>2</sub>) Batteries:** A reliable power source that can supply currents in the microampere range is essential for implantable cardiac pacemakers [34]. The lithium/iodine-polyvinylpyridine (PVP) system, patented for the first time in 1972, continues to serve as the power source for these devices today. For this application, Li/I<sub>2</sub>-PVP cells are the foremost option, owing to their high energy density, safety standards, and reliability. The cell reaction results in open circuit cell potential of 2.8V. The energy density of Li/I<sub>2</sub> batteries can reach 210 W·h/kg, which can power a cardiac pacemaker for several years.
- **Lithium/Manganese (Li/MnO<sub>2</sub>) Dioxide Batteries:** Biomedical devices, such as neurostimulators, drug delivery systems, and pacemakers with enhanced

capabilities, require batteries that can provide power in the milliwatt range. The Li/MnO<sub>2</sub> [35] primary battery, first introduced commercially in the 1970s, is a suitable option for these medium-rate applications. This battery system is widely recognized for its high operating cell potential, significant specific energy density, and excellent performance in both storage and discharge.

- **Lithium/ Carbon Monofluoride (Li/CF<sub>x</sub>) Batteries:** The lithium/carbon monofluoride (Li/CF<sub>x</sub>) system [36] offers an alternative for implantable biomedical devices that necessitate current outputs in the milliampere range. Initially developed in the early 1970s as a cathode material for lithium primary batteries, the Li-CF<sub>x</sub> system is recognized for its low self-discharge, high working cell potential, and considerable energy density, which enhance its utility as a medium-rate power source.
- **Lithium/Silver Vanadium Oxide (Li/SVO) Batteries:** Implantable cardioverter defibrillators (ICDs) are sophisticated medical devices that continuously monitor a patient's cardiac activity and detect instances of tachycardia, characterized by an accelerated heartbeat. Due to the substantial power requirements of ICDs, a battery capable of providing high current pulses of 2–3 A is essential for the rapid charging of the device's capacitors. Additionally, the battery must maintain a steady low current to support the heart monitoring functions of the ICD while also being able to deliver intermittent high current pulses throughout its operational lifespan within the patient. The lithium/silver vanadium oxide (Li/SVO) [37] battery system fulfils these criteria and is currently the most prevalent choice for ICDs.

### 1.5.2 Secondary (Rechargeable) Batteries

In a rapidly evolving healthcare landscape, the optimal selection is advanced battery technology that ensures safety, offers extended runtimes with reduced charging durations,

and is considerably lighter and more portable. The suitable battery type for medical instruments can vary according to the specific device and its power needs. However, rechargeable batteries, including lead-acid and lithium-ion, are commonly employed in medical devices because of their high energy density, extended cycle life, and ability to maintain consistent power output.

- **Lead-acid Battery:** The lead-acid battery presents numerous advantages when compared to other electrochemical energy sources. Its affordability and the widespread availability of lead contribute to its appeal. Additionally, it boasts a reliable performance, a cell voltage of 2 V, high electrochemical efficiency, and a cycle life ranging from several hundred to thousands of cycles. These characteristics make lead-acid batteries particularly suitable for medium to large-scale energy storage applications, as they provide an effective balance of power capabilities at a low cost. Typically, these batteries consist of multiple cells connected in series. The primary components of a lead-acid battery include electrodes, separators, electrolytes, containers with lids, ventilation systems, and various other elements [38].

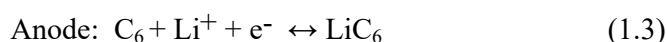
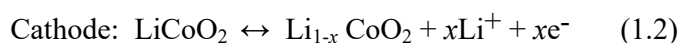
In a lead-acid battery, the active material consists of lead oxide (PbO) that is applied to a grid and subsequently undergoes electrochemical transformation into reddish-brown lead dioxide (PbO<sub>2</sub>) at the positive electrode, while the negative electrode is composed of grey spongy lead (Pb). Separators are employed to electrically isolate the positive electrode from the negative one, and an aqueous solution of sulfuric acid (H<sub>2</sub>SO<sub>4</sub>) serves as the electrolyte, with a density ranging from 1.22 to 1.28 g/cm<sup>3</sup> [39].

Overall chemical reaction during discharge is:



The reaction proceeds in opposite direction during charge.

- **Lithium-ion Batteries:** Lithium-ion batteries have been pivotal in facilitating the portable electronics revolution over the last three decades. Currently, these batteries function by employing reversible lithium-ion intercalation within both the cathode and anode to effectively store energy. Although the electrochemical insertion of lithium into transition metal compounds was documented in the 1970s, it was not until the advent of lithiated transition metal oxides and the intercalation of lithium into graphite that the first commercially viable battery was introduced by Sony. The fundamental structure of a lithium-ion battery is illustrated in **Fig. 1.5**, where the cathode material is typically  $\text{LiCoO}_2$  and the anode is composed of graphite. The advantage of utilizing these two electrode materials is that they result in a high cell voltage of 3.6 V and an energy density of approximately  $120\text{-}150 \text{ Wh kg}^{-1}$  [40]. The electrolyte is  $\text{LiPF}_6$  in a mixture of organic solvents such as ethylene carbonate and dimethyl carbonate. The reactions during the energy-storage (charging) stage are:



These reactions are reversed during the discharge cycle; commercial lithium-ion batteries are rated for approximately 500 charge/discharge cycles [41].

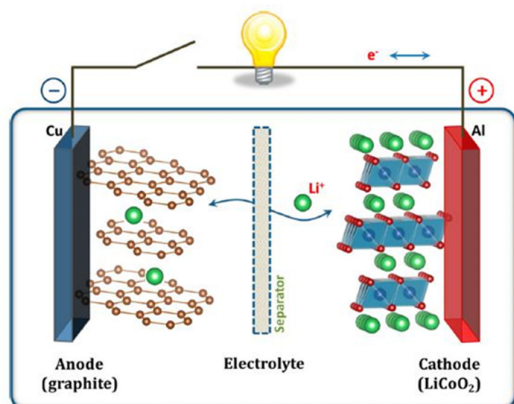


**Figure 1.5-** The configuration of a rechargeable Li-ion battery (Figure is taken from open access internet source)

### 1.5.3 Other Batteries

The first implantable pacemaker in 1960 was powered by the Ruben Zn/HgO cell [42]. On the other hand, Bio-fuel cells are devices that convert biochemical energy into electrical energy through electrochemical reactions that utilize biochemical pathways [43]. The connection between biological processes and electricity was first identified by Galvani in 1791. The term 'fuel cell' was introduced in 1839 when Grove successfully reversed the electrolysis of water, recombining oxygen and hydrogen to generate water along with an electrical current [44]. The advancement of microbial fuel cells (MFC) began in 1911 when Potter discovered that a current of 0.2–0.5 mA at 0.3–0.5 V could be produced by inserting a platinum electrode into *E. coli* cultures [45], highlighting the potential of microorganisms for power generation. This concept was further demonstrated in 1931 by Cohen, who created biofuel cells that generated 2 mA of current and 35 V of voltage [46]. In a fuel cell, oxidation and reduction reactions take place at the anode and cathode, respectively. The electrons released during oxidation travel to the cathode, creating an electrical current through an external circuit, while protons migrate to the cathode via a proton-selective exchange membrane [47].

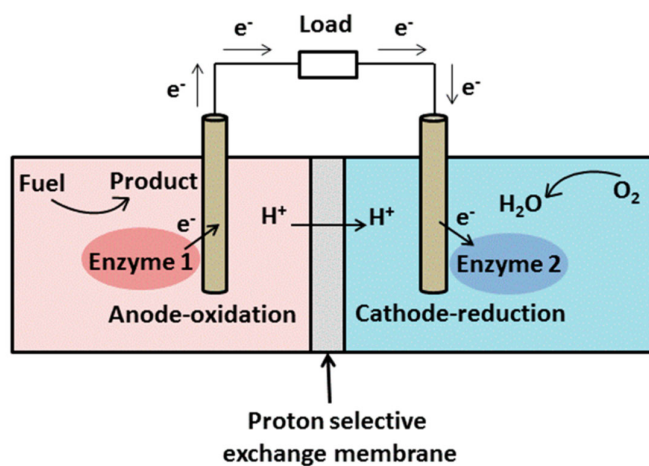


**Figure 1.6-** Diagram illustrating a bio-fuel cell (Figure is taken from open access internet source).

## 1.6 Limitations of existing systems and new requirements

Lead-acid batteries have several disadvantages [48], including:

- The lead-acid battery has one of the lowest energy densities, making it unsuitable for portable devices. Lead-acid batteries only have 30% to 50% of their energy useable.
- The optimum operating temperature for the lead-acid battery is 25°C (77°F). Elevated temperature reduces longevity. As a guideline, every 8°C (15°F) rise in temperature cuts the battery life in half.
- Lead-acid batteries are very corrosive and can burn skin, especially if they are acidic.
- Charging lead-acid batteries can be expensive for businesses. Lead-acid batteries can take a long time to charge, especially when recharging the final 20% of the battery.
- Transportation restrictions on flooded lead acid - there are environmental concerns regarding spillage. Lead content and electrolyte make the battery environmentally unfriendly.
- Lead-acid batteries have a short cycle lifespan and overall lifespan. They typically need to be replaced every five years.

Li-ion batteries, while technologically advanced, exhibit several limitations, especially concerning safety. These batteries are prone to overheating and may sustain damage when subjected to high voltages. Such conditions can occasionally result in thermal runaway and combustion [49]. Additionally, Li-ion batteries experience aging, leading to a reduction in capacity and an increased likelihood of failure after a few years of use. Their cost, approximately 40% higher than alternatives, further restricts their broader implementation.

Moreover, they are not optimally designed for applications necessitating rapid charge storage, such as regenerative braking [50].

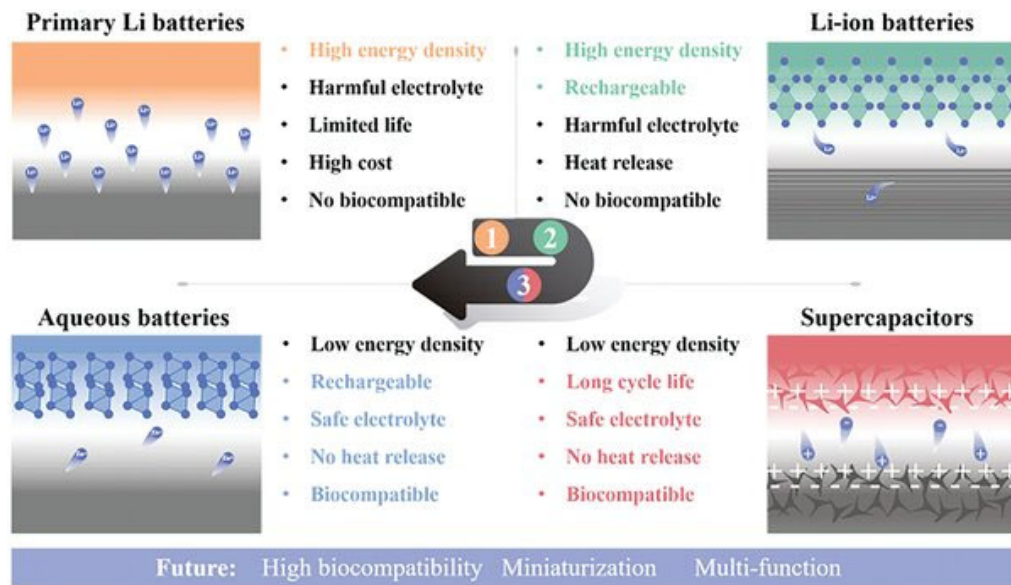


**Figure 1.7-** Overview of energy storage devices. ((Figure is taken from open access internet source)

Significant progress has been achieved over the past few decades in enhancing battery performance; however, the primary challenge lies in peak usage. Even in compact electronic devices like smartphones and laptops, batteries can sustain damage due to abrupt energy demands. This issue is particularly prevalent in electric vehicles (EVs), where various factors, including driving behaviour and road conditions, lead to swift fluctuations in power consumption. A battery operates optimally when it is discharged in a steady manner, as this allows the associated electrochemical reactions to occur uniformly. When an electric vehicle (EV) experiences a sudden demand for power during acceleration, the battery pack is often unable to discharge at a rate sufficient to meet this need. This limitation also applies to the high current generated during the vehicle's braking process. The rapid fluctuations of high electric current entering and exiting the battery can adversely affect the electrolytes. In scenarios where acceleration and braking occur frequently, such as in urban driving, the lifespan of the batteries may be significantly reduced. Consequently, there is a

pressing need for alternatives to address issues related to battery longevity and power output. The current situation necessitates a device with specialized capabilities, including high power, energy density, and extended cycle life [51]. Modern high-power applications require substantial energy and rapid delivery, which batteries and capacitors alone cannot adequately provide [52]. In response to these challenges, supercapacitors have been developed over the past few decades to meet the essential demands of traditional energy storage devices, such as batteries and capacitors.

### **1.6.1 Understanding the problem**

The challenge of developing a large-scale energy storage solution that effectively addresses the following issues remains significant:

- Limited power output despite high energy storage capacity
- Lack of immediate responsiveness
- High Internal impedance
- Reduced lifespan with property degradation
- Compact size requirements
- Concerns regarding flammability and safety hazards.

It is clear that achieving all of these features within a single device is not feasible unless we possess an extraordinary storage solution [53-54]. However, we can implement trade-offs to enhance performance for specific applications, and we can persist in making innovative advancements.

Significant emphasis in the energy storage device sector is placed on the creation of a grid-scale bulk energy storage and distribution system that possesses enhanced energy storage and power delivery capabilities. Consequently, Redox flow batteries, Metal-air batteries, and Hybrid supercapacitors are of considerable technological importance, with materials

development aimed at improving their performance being a primary focus within the energy materials domain.

### 1.6.2 Electrochemical Supercapacitors

Electrochemical supercapacitors (ESs) are emerging energy storage devices that offer a balance of power and energy performance and bridge the gap between conventional capacitors and batteries [55-57]. In addition to their performance characteristics, ESs offer several benefits, including an extended cycle life and rapid charge-discharge capabilities, rendering them ideal for applications that are beyond the reach of both capacitors and batteries. Presently, ESs are utilized in electric vehicles alongside batteries, demonstrating their ability to minimize the overall dimensions of the power source, enhance battery longevity, and decrease energy losses.

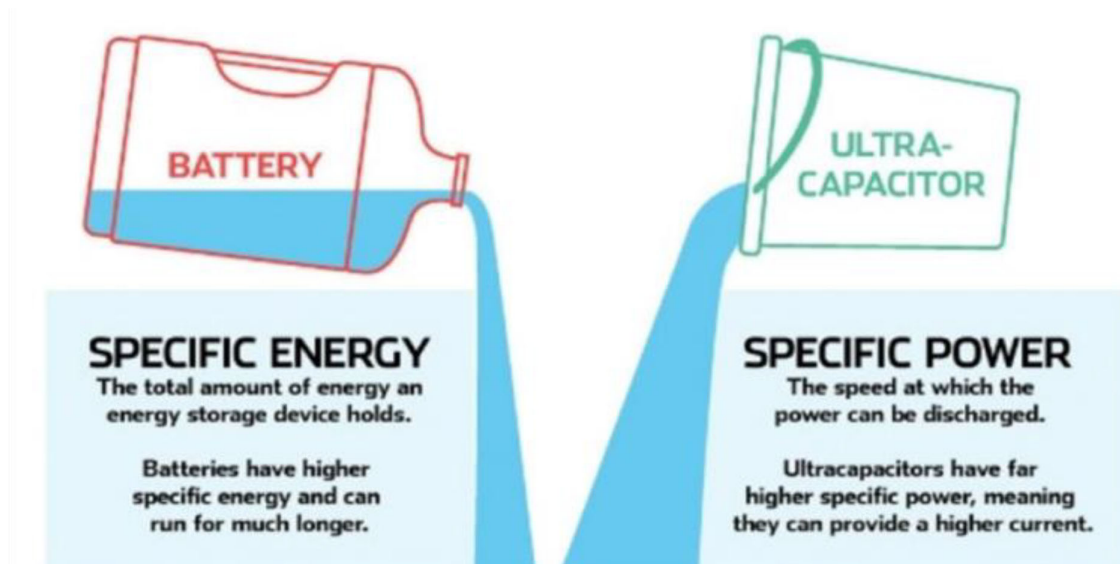


**Figure 1.8-** Advantage of supercapacitors over battery. (Figure is taken from open access internet source)

A supercapacitor (SC), also called an ultracapacitor, is a high-capacity capacitor with a capacitance value much higher than other capacitors but with lower voltage limits that bridge the gap between electrolytic capacitors and rechargeable batteries. It typically stores

10 to 100 times more energy per unit volume or mass than electrolytic capacitors, can accept and deliver charge much faster than batteries, and tolerates many more charge and discharge cycles than rechargeable batteries [58]. Unlike ordinary capacitors, supercapacitors do not use the conventional solid dielectric, but rather, they use electrostatic double-layer capacitance and electrochemical pseudo capacitance, both of which contribute to the total capacitance of the capacitor, with a few differences.

ESs can be classified into two categories based on the charge storage mechanism [59]: (i) Electrochemical double-layer capacitors (EDLCs) and (ii) Pseudocapacitors.

### 1.6.3 Electrochemical double-layer capacitors

In Electric Double Layer Capacitors (EDLCs), the mechanism of charge and discharge is based on the accumulation and separation of electrostatic charges at the interface between the electrode and the electrolyte on both electrodes, as illustrated in **Fig. 1.9**. The capacitance resulting from this interface is referred to as double-layer capacitance (Cdl) [60]. Like traditional capacitors, EDLCs are composed of positive and negative electrodes submerged in an electrolyte; however, they provide a greater capacitance per unit volume by utilizing high surface area porous carbon materials as the active components.

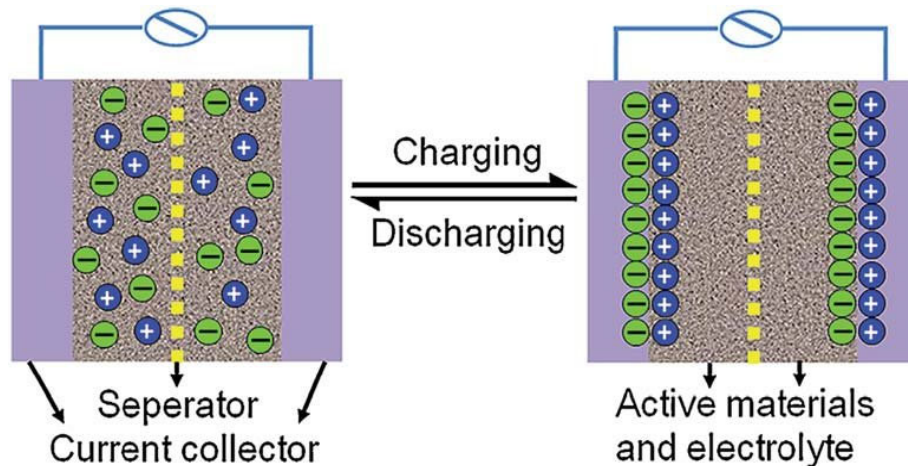


**Figure 1.9-** The charge storage mechanism of EDLC. (Figure is taken from open access internet source)

## 1.6.4 Pseudocapacitors

In electric double-layer capacitors (EDLCs), energy storage relies on the accumulation of charge at the electrode surface. Conversely, pseudocapacitors store energy through rapid and reversible redox reactions occurring at the surfaces of active materials. When compared to EDLCs, pseudocapacitors provide capacitance that is 10 to 100 times greater, as charge storage extends beyond the surface to include the near-surface region where ions are capable of diffusing [61]. Nevertheless, the slower faradic processes limit the power performance of pseudocapacitors in comparison to EDLCs.

Pseudocapacitance arises when electrode potential is dependent logarithmically on the extent of reactions and involves charge transfer across the double layer. Conway has identified faradic systems that can give rise to pseudocapacitance: (i) underpotential deposition system, (ii) redox pseudocapacitance, and (iii) intercalation pseudocapacitance [62].

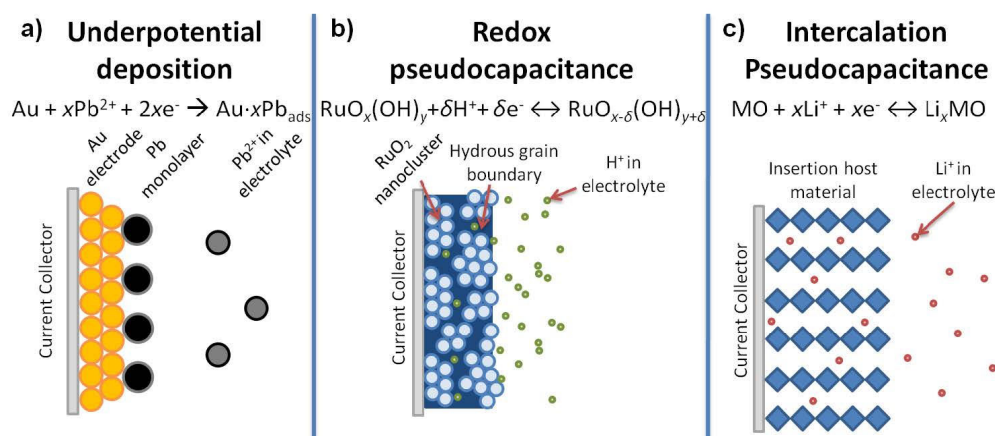


**Figure 1.10-** Schematic of pseudocapacitive systems identified by Conway (Figure is taken from open access internet source)

## 1.6.5 Hybrid battery-type supercapacitor

A hybrid battery type supercapacitor, referred to as a hybrid supercapacitor (HSC) device also, is an electrochemical energy storage system that integrates the benefits of both

supercapacitors and rechargeable batteries [63, 64]. In a hybrid supercapacitor, the processes of electrical double-layer capacitance and faradaic or battery capacitance occur concurrently. The electrodes that utilize redox or battery-type mechanisms exhibit a significant energy density, whereas the nonfaradaic capacitive electrode is characterized by a high-power density and remarkable cycling stability.

The initial concept for hybrid supercapacitors (HSCs) was developed in the mid-1990s, introducing a device constructed from fibrous carbon material and nickel oxide as electrodes. This innovation demonstrated an 8 to 10-fold increase in capacity compared to traditional double-layer capacitors. This prototype established a foundational framework for the construction of HSC devices, integrating a battery-type electrode with a capacitive-type electrode to facilitate the electrochemical interactions between the two. Both types of electrodes can function as either anode or cathode. The essential configuration of HSCs is illustrated in **Fig. 1.11**.

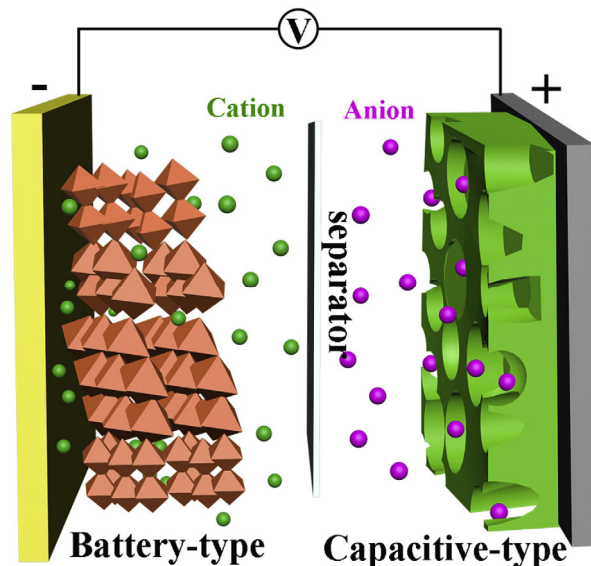


**Figure 1.11-** The fundamental configuration of the HSCs (Figure is taken from open access internet source)

In the electrochemical process, a battery-type electrode accumulates energy through Faradaic charge transfer, while the complementary electrode maintains charge balance by

electrosorbing guest ions onto the surface of the active material, such as activated carbon. Within the same device, two distinct electrochemical processes—Faradaic and non-Faradaic reactions—occur concurrently. The former electrode, characterized by well-defined redox peaks, functions as the energy output source, although it exhibits limitations in rate capability and cycling longevity. In contrast, the latter electrode does not engage in Faradaic charge transfer; instead, it stores charge solely at the surface in the form of a double layer, allowing for a rapid response to potential fluctuations, thereby contributing to power output. Additionally, the electrochemical kinetics of battery-type and capacitive-type electrodes differ significantly and can be articulated through the following equation [65-78].

$$i = Cv^b \quad (1.4)$$

where  $i$  is the current and  $v$  is the scan rate of a cyclic voltammetry (CV) curve. The battery-type material with  $b = 0.5$  has a diffusion-controlled electrochemical behaviour, while the  $b$  value of capacitive-type material approaches to 1 due to its surface-controlled electrochemical behaviour.

## 1.7 Electrode materials

Enhanced supercapacitive performance can be attained by choosing active materials with specific characteristics. The properties of the active material are crucial in realizing superior supercapacitive performance. The majority of the materials employed in the development of the SC cell exhibit biocompatibility [69-71]. This characteristic is vital for medical devices, as it ensures that they do not cause harm or provoke an immune response. SCs are recognized for their exceptional reliability and long-term stability.

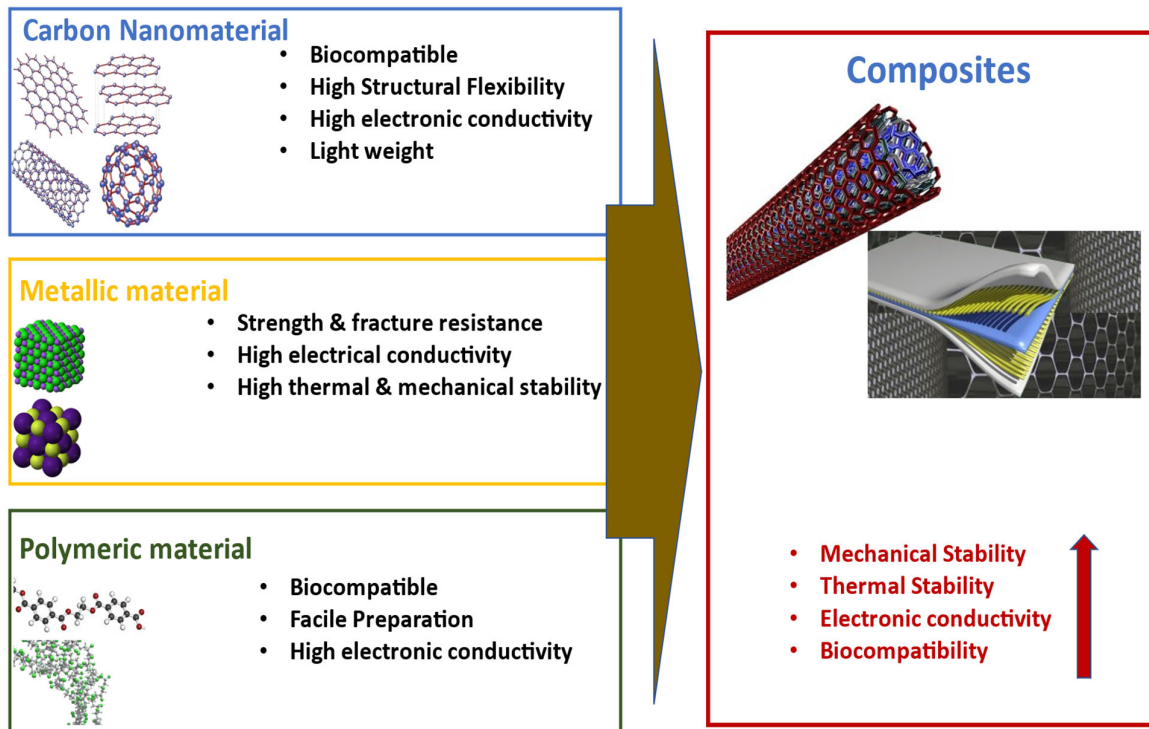


**Figure 1.12-** Properties of active materials including carbon nanomaterials, conducting polymers, metal and metal oxides, and composites

They demonstrate a reduced susceptibility to capacity degradation, a common issue in rechargeable batteries [72, 73]. The combination of high reliability and excellent cyclic stability is critical for implantable devices that are required to operate consistently over prolonged durations. Metal oxides and hydroxides are used as active materials for pseudocapacitors, which have high theoretical capacitances originating from fast faradic reactions and resulting in a much higher energy density than EDLCs. Many metal oxides and hydroxides such as  $\text{RuO}_2$ ,  $\text{MnO}_2$ ,  $\text{V}_2\text{O}_5$ ,  $\text{NiO}$ ,  $\text{Co}_3\text{O}_4$ ,  $\text{Fe}_2\text{O}_3$ , and  $\text{FeOOH}$  are some examples of materials, which have been investigated and have shown exceptional results as active materials for ESs. However, the majority of these metal oxides and hydroxides suffer from low electrical conductivity, and conductive carbon materials are incorporated to fabricate composite materials [74]. A review of electrodes developed till now is presented below

### **1.7.1 Carbon-based Electrode materials**

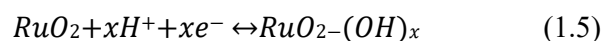
A diverse range of carbon nanomaterials has gained significant popularity in the preparation of electrode materials for various energy storage devices. In the context of supercapacitors (SCs), specific carbon allotropes such as activated carbon (AC), carbon nanotubes (CNTs), graphene (Gr), carbon nanocages (CNCs), and carbon nanofibers (CNFs) have been employed. The primary rationale for the utilization of carbon-based nanomaterials in SC applications lies in their chemical inertness and thermal stability, which contribute to exceptional cyclic stability and power performance in SC devices. Each of these carbon allotropes offers distinct advantages for supercapacitors. For instance, activated carbon is characterized by a high specific surface area, favorable electronic conductivity, cost-effectiveness, and reliable cyclic performance [75-77]. Specifically, each of these carbon allotropes has unique advantages for SCs. For example, AC has a large specific surface area (SSA), good electronic conductivity, low cost, and stable cyclic performance [78, 79]. 1D CNTs are extensively explored for SCs due to their 1D nature, regular pore structure, high conductivity, and significant SSA.

### **1.7.2 Metal Oxides Composite Electrodes**

Metallic substances, including metals, metal oxides, and alloys, were originally utilized as biomaterials for implants. In contemporary practice, these materials are widely applied across various fields due to their ability to offer significant strength and resistance to fracture [80]. Additionally, due to their exceptional thermal and mechanical stabilities, these materials are capable of adjusting to swift alterations in the bodily environment, including variations in temperature and pressure. Furthermore, their efficiency in transferring thermal energy and electrical charge is significantly enhanced by the presence of free electrons [81].

### 1.7.2.1 Ruthenium dioxide (RuO<sub>2</sub>)

Ruthenium dioxide is among the earliest metal oxides studied for its potential use in electrochemical systems. Both its crystalline and amorphous hydrous forms exhibit optimal characteristics for faradic active materials, including multiple oxidation states, elevated electrical and ionic conductivities, as well as excellent cyclic stability [74]. In 1971, Trasatti and colleagues synthesized a RuO<sub>2</sub> thin film through thermal decomposition, which demonstrated capacitive characteristics when immersed in a 1M HClO<sub>4</sub> electrolyte within a voltage range of 0 to 1.45V relative to the reversible hydrogen electrode (RHE) [82]. Under acidic conditions, the charge storage mechanism of RuO<sub>2</sub> can be described by Equation 1.5.



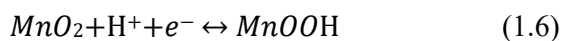
The pseudocapacitance of RuO<sub>2</sub> thin film was attributed to the successive redox transition from Ru<sup>2+</sup> to Ru<sup>4+</sup>, and the conversion of OH<sup>-</sup> to O<sup>2-</sup> within the structure by transfer of proton [53]. The performance of RuO<sub>2</sub> electrodes is governed by the charge transfer and diffusion processes, such as electron hopping within and between RuO<sub>2</sub> particles, electron transfer from active materials to current collectors, and ion diffusion within RuO<sub>2</sub> [83]. Among the two forms of RuO<sub>2</sub>, the hydrous form of RuO<sub>2</sub> has shown higher capacitance compared to the anhydrous. Sugimoto et al. have investigated the capacitive performance of RuO<sub>2</sub> with different water content, and they have shown anhydrous RuO<sub>2</sub> has a much lower capacitance (24 Fg<sup>-1</sup>) than the hydrous form (342 Fg<sup>-1</sup>) [84] and explained with the tree root model for anhydrous RuO<sub>2</sub>, the particles are agglomerated with no available micropores for ion diffusion, and hydrous RuO<sub>2</sub> particles are smaller, and hydrated micropores exist between particles allowing good ion transport. Therefore, the water

content in RuO<sub>2</sub> plays an important role, which is responsible for fast ionic conduction through the porous structure to enhance capacitive performance.

Despite having the ideal properties for ESs applications, the high cost of RuO<sub>2</sub> has limited its applications. To address this problem, some research was conducted to fabricate RuO<sub>2</sub> composite with low-cost metal oxides or deposition of RuO<sub>2</sub> on conductive substrates. Hu et al. have fabricated hydrous RuO<sub>2</sub> – TiO<sub>2</sub> nanocomposite by hydrothermal process, and such electrodes have shown remarkable capacitance of 992 F g<sup>-1</sup> at the scan rate of 100 mV s<sup>-1</sup> [85]. In another study by Hsieh et al., composite composed of vertically aligned MWCNTs coated with hydrous RuO<sub>2</sub> on a titanium current collector, and a maximum capacitance of 1652 F g<sup>-1</sup> was achieved [86].

#### 1.7.2.2 Manganese dioxide (MnO<sub>2</sub>)

Manganese dioxide (MnO<sub>2</sub>) has been the subject of extensive research for energy storage applications, attributed to its high theoretical capacitance of 1370 F g<sup>-1</sup>, affordability, lower toxicity in comparison to other metal oxides, and the presence of multiple oxidation states [87,88]. Similar to RuO<sub>2</sub>, the pseudocapacitance of MnO<sub>2</sub> is derived from the successive redox transition of Mn<sup>3+</sup> and Mn<sup>4+</sup>, and the charge storage mechanism can be expressed by Eq.1.6.



One benefit of MnO<sub>2</sub> in comparison to RuO<sub>2</sub> is its ability to function effectively in a mild aqueous electrolyte, such as Na<sub>2</sub>SO<sub>4</sub> and chloride salts (KCl, NaCl), rather than requiring the strong acid or base electrolytes that are utilized in RuO<sub>2</sub> systems.

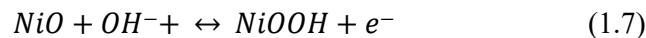
MnO<sub>2</sub> has various crystal structures, denoted by  $\alpha$ ,  $\beta$ ,  $\gamma$ ,  $\delta$ , and  $\lambda$  phases, and is a crucial factor in the electrochemical performance of MnO<sub>2</sub>, and all phases have tunnel structures for electrolyte access, where the tunnel size varies from 1.89 to 7 Å. Brousse et al. and

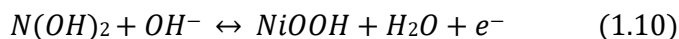
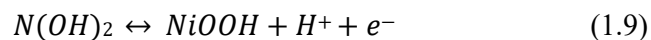
Devaraj et al. have determined the capacitance of different structures of MnO<sub>2</sub> in a 0.1M K<sub>2</sub>SO<sub>4</sub> and 0.1M Na<sub>2</sub>SO<sub>4</sub> solution respectively, and both authors suggested that the capacitance of MnO<sub>2</sub> decreases in the order of  $\alpha \cong \delta > \gamma > \lambda > \beta$ .

In a separate investigation conducted by Ghodbane et al., the surface area of various MnO<sub>2</sub> structures was examined to explore the relationship between surface area and capacitance. The findings indicated that the capacitance of MnO<sub>2</sub> is more closely related to ionic conductivities than to the BET surface area [89]. The findings suggest that the charge storage mechanism of MnO<sub>2</sub> extends beyond mere surface reactions to include ion intercalation within the bulk of MnO<sub>2</sub>.

### 1.7.2.3 Nickel oxide (NiO) & nickel hydroxide (Ni(OH)<sub>2</sub>)

NiO represents a highly promising option for energy storage applications, attributed to its remarkably high theoretical capacitance of 2584 F g<sup>-1</sup>, affordability, and low toxicity [90]. NiO is generally produced by first creating Ni(OH)<sub>2</sub>, which is then subjected to high-temperature annealing to yield NiO. [83]. The electrolyte utilized for the NiO electrode typically consists of alkaline solutions; however, the mechanism of charge storage remains ambiguous. Two theories have been proposed regarding the pseudocapitance of NiO in alkaline environments. The first theory suggests that redox reactions occur between NiO and nickel oxyhydroxide (NiOOH) (Eq.1.7 & 1.8), while the second theory posits that the reactions take place between Ni(OH)<sub>2</sub> and NiOOH (Eq.1.9 & 1.10) [88]. However, it is commonly believed that Eq.1.7 occurred first to produce NiOOH, followed by the reversible redox reactions between Ni(OH)<sub>2</sub> and NiOOH[67].





There are several challenges associated with NiO, including a notably lower specific capacitance than the theoretical maximum, limited electrical conductivity, and inadequate cyclic stability [88]. Similar to other metal oxides, efforts have been focusing on fabricating nanostructured NiO or NiO composite with other materials [91, 92]. Nam et al. conducted a study on the electrochemical characteristics of a porous NiO film, which was produced from an electroplated Ni(OH)<sub>2</sub> film on a nickel foil substrate, utilizing various deposition current densities followed by thermal treatment. Their findings revealed that the specific capacitance of the NiO film improved with an increase in deposition rate, ultimately reaching a specific capacitance of 277 F g<sup>-1</sup> in a 1M KOH electrolyte for the NiO film deposited at a current density of 4 mA cm<sup>-2</sup> [93]. In another investigation by Yuan et al., they fabricated porous NiO nano and microspheres to improve rate performance. The approach involved a low-temperature precipitation reaction with an alkaline solution and nickel salts, and the fabricated electrode exhibited a specific capacitance of 525F g<sup>-1</sup> at the current density of 4 A g<sup>-1</sup>[94]. The hierarchical porosity created by the nano and microspheres has resulted in an impressive capacitance retention of 98% following 2000 cycles.

Ni(OH)<sub>2</sub> has a hexagonal layered structure with two polymorphs, α-Ni(OH)<sub>2</sub> and β-Ni(OH)<sub>2</sub>, and have been demonstrated that the structure has an impact on the performance of the electrodes[95]. α-Ni(OH)<sub>2</sub> has intercalated with anions and water within the structure, whereas water is absent in β-Ni(OH)<sub>2</sub>[74]. The α-Ni(OH)<sub>2</sub> showed a higher specific capacitance than β-Ni(OH)<sub>2</sub>, and the situation can be explained by recalling that

hydrous RuO<sub>2</sub> showed higher specific capacitance than the anhydrous form due to improved ion transport[84, 96].

### **1.7.3 Conductive Polymers Composite Electrodes**

Conducting polymers (CPs) represent a noteworthy subclass of materials for supercapacitors, attributed to their excellent conductivity, substantial charge storage capacity, straightforward synthesis process, affordability, and eco-friendliness, a recognition that has been in place since their discovery in 1976. [97,98] The capacitive characteristics of conducting polymers typically arise from the reversible redox reactions involving the  $\pi$ -conjugated double bonds within the polymer networks, facilitated by doping and dedoping processes. In recent years, various CPs, including polypyrrole (PPy), polyaniline (PANI),[99] polythiophene (PTh), poly(3,4-ethylenedioxythiophene) (PEDOT) [100], and their derivatives have been developed and investigated in SCs. However, due to the poor conductivity, the PANI, PPy,[101] and PTh[102] possessed low specific capacitances of 150–190, 80–100, and 78–117 F g<sup>-1</sup> in both aqueous and non-aqueous electrolytes, respectively. The inferior electrochemical stability of these materials, resulting from structural degradation caused by the expansion and contraction of conducting polymers during the intercalation and deintercalation processes, significantly restricts their use in high-performance supercapacitors.

## **1.8 Our Electrode development approach**

Metal-organic frameworks (MOFs) exhibit a unique open framework architecture, formed by the combination of metal-containing components and organic linkers, which are held together by robust bonds that ensure permanent porosity. Highly porous metal oxalate frameworks demonstrate characteristics akin to battery-type faradaic pseudocapitance. A reversible mechanism involving surface redox and ion intercalation reactions has been

identified for charge storage in a material that incorporates an active redox couple facilitating charge transfer.

In our study, we synthesized oxalate and phosphate-based material for electrode development and conducted electrochemical investigations. In addition to the experimental methodology, we also conducted an investigation utilizing machine learning algorithms to identify novel electrode materials.

### 1.8.1 Transition metal oxalate-based electrodes

In addition to transition metal oxides, oxalate-based metal-organic frameworks (MOFs) have demonstrated efficacy as active materials for energy storage systems. MOFs offer several benefits, including high energy density, low toxicity, affordability, a stable pore structure, and a broad potential window due to the presence of multiple oxidation states [103]. and the charge storage mechanism is described by eq.1.11.



Wang et al. have to synthesize  $\text{Ni}_{0.55}\text{Co}_{0.45}\text{C}_2\text{O}_4$  solid solution by the liquid-liquid interfacial reaction involving a co-precipitation process and get a micro-cuboid structure composed of nanoparticles with sizes ranging from 13 to 23 nm. Moreover, electrochemical measurements achieved a specific capacity of  $562 \text{ C g}^{-1}$  at a current density of  $1 \text{ Ag}^{-1}$  [104]. In another investigation, Zhao et. al. demonstrated the use of (Ni-OA) for ESs application. They prepared the electrode 2D porous Ni-OA thin sheets by the direct hydrothermal decomposition of a mixed aqueous solution of transition metal nitrates  $\text{Ni}(\text{NO}_3)_2$  and OA. The fabricated electrode was tested in a 6 M KOH electrolyte and showed a specific capacitance of  $2835.06 \text{ F.g}^{-1}$  at  $1.0 \text{ Ag}^{-1}$ . The cyclic stability of the electrode was also tested (94.3 % of capacity retention after 5,000 cycles at  $10 \text{ A.g}^{-1}$ ) [105]. Pu et. al. have synthesized 2D porous Co-OA thin sheets with different sizes and crystallinity assembled

by interconnected nanosheet frameworks by hydrothermal strategy at 220 °C for different reaction times. The electrode was tested in a 6 M KOH electrolyte and showed specific capacitance ( $1.631 \text{ F}\cdot\text{cm}^{-2}$  at the current density of  $1.2 \text{ mA}\cdot\text{cm}^{-2}$ . the retention rate was 80.6 % when the current density increased 10 times [87]. Cheng et. al. has synthesized nanostructured cobalt oxalate electrodes by one-step in-situ electrochemical method (anodization). The prepared electrode was demonstrated in KOH electrolyte and showed a specific capacitance of  $1269 \text{ F g}^{-1}$  at the current density of  $6 \text{ A g}^{-1}$  in the galvanostatic charge/discharge test. Moreover, the electrode also tested rate capability and cycling stability (8.1% decay after 100,000 cycles) [106],

### **1.8.2 Metal phosphate-based materials for high-performance supercapacitors**

Metal phosphates, especially the layered metal phosphonates and phosphates, attracted significant interest from the research community between 1987 and 1990 [107]. They demonstrate exceptional capabilities in various fields, including catalysis, ion exchange, proton conductivity, interface chemistry, photochemistry, and materials science.[108, 109] Carling and Yuan et al. obtained  $\text{NH}_4\text{M}^*\text{PO}_4\cdot\text{H}_2\text{O}$  ( $\text{M}^* = \text{Mn, Fe, Co, and Ni}$ ) by precipitation from aqueous solution.[97,98] Zhang et al. [99] successfully prepared metal ammonium phosphate microspheres. Additionally, Li et al. developed amorphous colloidal spheres derived from transition-metal phosphates [110]. Transition metal phosphates, such as nickel and cobalt phosphates, have the potential to serve as effective anodes in various applications, including sorbents, magnetic materials, rechargeable batteries, ion exchangers, and heterogeneous catalysts. Meanwhile,  $\text{PO}_4$  polyhedra with a zeolite structure have outstanding electronic and magnetic properties. Hence, these materials have attracted great attention.

### 1.8.3 Existing electrode materials and their energy storage capacity

The table below illustrates the energy storage capacity associated with most of the transition metal oxides and metal oxalated based electrode materials that are presently utilized.

<b>Values of specific capacitance of some transition-metal oxides</b>				
<b>Material</b>	<b>Specific Capacitance (F g<sup>-1</sup>)</b>	<b>Current Density</b>	<b>Electrolyte</b>	<b>Ref.</b>
RuO <sub>2</sub> .nH <sub>2</sub> O	720	-	Strong H <sub>2</sub> SO <sub>4</sub>	127
RuO <sub>2</sub> film on silicon wafer	275	1.4 mA cm <sup>-2</sup>	1M H <sub>2</sub> SO <sub>4</sub>	128
amorphous MnO <sub>2</sub> .nH <sub>2</sub> O	200	2 mA cm <sup>-2</sup>	2M KCl	129
α-MnO <sub>2</sub>	297	0.5 mA cm <sup>-2</sup>	0.1M Na <sub>2</sub> SO <sub>4</sub>	130
β-MnO <sub>2</sub>	9	0.5 mA cm <sup>-2</sup>	0.1M Na <sub>2</sub> SO <sub>4</sub>	130
Porous NiO	50	20 mV s <sup>-1</sup>	1M KOH	131
Amorphous V <sub>2</sub> O <sub>5</sub>	350	2 mA cm <sup>-2</sup>	2M KCl	132
Co <sub>3</sub> O <sub>4</sub>	746	5 mA cm <sup>-2</sup>	6M KOH	133
Co <sub>3</sub> O <sub>4</sub>	358	2 A g <sup>-1</sup>	KOH	134
Fe <sub>3</sub> O <sub>4</sub>	170	2 mV s <sup>-1</sup>	1M Na <sub>2</sub> SO <sub>3</sub>	134
Fe <sub>3</sub> O <sub>4</sub>	3	2 mV s <sup>-1</sup>	1M KOH	135
Porous NiO <sub>2</sub> O <sub>4</sub>	1089	2 A g <sup>-1</sup>	2M KOH	136
Doped-SrRuO <sub>3</sub>	160	20 mV s <sup>-1</sup>	6M KOH	137
LaNiO <sub>3</sub>	160	10 mV s <sup>-1</sup>	1M Na <sub>2</sub> SO <sub>4</sub>	138
LaMnO <sub>2.91</sub>	610	1 mV s <sup>-1</sup>	1M KOH	139
La <sub>0.7</sub> Sr <sub>0.3</sub> CoO <sub>3-δ</sub>	748	2 A g <sup>-1</sup>	1M Na <sub>2</sub> SO <sub>4</sub>	140
Ni-doped Mn <sub>3</sub> O <sub>4</sub>	704	10 mV s <sup>-1</sup>	1M Na <sub>2</sub> SO <sub>4</sub>	141
Mn-incorporated MoS <sub>2</sub>	430	5 mV s <sup>-1</sup>	0.5M Na <sub>2</sub> SO <sub>4</sub>	142
Pyrite FeS <sub>2</sub> nanobelts	308	5 mV s <sup>-1</sup>	1M Na <sub>2</sub> SO <sub>4</sub>	143
(Ni <sub>0.33</sub> Co <sub>0.67</sub> )Se <sub>2</sub> complex	828	1 A g <sup>-1</sup>	3M KOH	144
SrFeO <sub>3-δ</sub>	733	1 mV s <sup>-1</sup>	-	145
SrFeO <sub>3-δ</sub>	741	1 A g <sup>-1</sup>	2M KOH	145
<b>Values of specific capacitance of some Metal-oxalate-based electrode materials</b>				
NiC <sub>2</sub> O <sub>4</sub> · 2H <sub>2</sub> O	990	-	2M KOH	146
NiC <sub>2</sub> O <sub>4</sub>	2835	1 A g <sup>-1</sup>	6M KOH	147
Anhydrous CoC <sub>2</sub> O <sub>4</sub>	2116	1 A g <sup>-1</sup>	2 M KOH	148
MnC <sub>2</sub> O <sub>4</sub> /GO	122	0.5 A g <sup>-1</sup>	6M KOH	149
FeC <sub>2</sub> O <sub>4</sub> /rGO hydrogel	591	2 A g <sup>-1</sup>	1M Na <sub>2</sub> SO <sub>4</sub>	150
Anhydrous Co <sub>0.5</sub> Ni <sub>0.5</sub> C <sub>2</sub> O <sub>4</sub>	2409	1 A g <sup>-1</sup>	2M KOH	151
Anhydrous NiC <sub>2</sub> O <sub>4</sub>	1638	1 A g <sup>-1</sup>	2M KOH	152
CoC <sub>2</sub> O <sub>4</sub>	1269	6 A g <sup>-1</sup>	2M KOH	153

*Table 1.1: Energy storage performance of some currently used electrode materials*

#### **1.8.4 Machine learning-inspired modelling of electrode**

Data-driven materials science leverages extensive data gathered from traditional theoretical and experimental techniques to investigate the mechanisms that drive material performance through the application of data-driven artificial intelligence (AI) methods. This approach minimizes the costs associated with trial and error in experiments as well as the expenses related to density functional theory (DFT) calculations typical of conventional methods, thereby conserving time that would otherwise be spent on repetitive experiments. [111]. Currently, machine learning (ML) stands as a prominent example of artificial intelligence techniques, serving as an innovative approach for identifying predictive rules. It has found extensive application in the prediction of material performance and the discovery of new materials. [112-114]. In the domain of batteries, encompassing a range of materials including cathodes, anodes, and electrolytes, as well as the intricate interactions among these components, machine learning offers researchers significant insights for the design and enhancement of rechargeable battery materials. [115]. The intricate characteristics of each material within a battery significantly influence its overall performance through their synergistic interactions. Given the variety of properties exhibited by different materials, it is nearly unfeasible for manual experimentation to explore all possible combinations and identify the optimal formulation. Machine learning leverages the substantial computational power and storage capabilities of computers to predict the properties of untested materials by analyzing existing experimental data. This approach offers clear direction and robust support for manual experimentation. Additionally, machine learning can extract valuable insights from both theoretical and experimental datasets [116].

Recently, machine learning techniques have garnered significant attention due to their efficacy in predicting physical and chemical properties [117, 118], conducting high-throughput screening for crystal structure prediction [119], uncovering the relationships

between structure and properties [120], and accelerating the chemical synthesis of high-performance materials [121-123]. An increasing focus has been placed on the application of machine learning models to accurately predict material properties. Chen et al. [124] presented machine learning applications aimed at predicting properties and advancing materials for energy storage and conversion systems, including catalysis, lithium-ion batteries, solar cells, and carbon dioxide capture, among others. Guan et al. [125] provided a comprehensive overview of the utilization of machine learning-based atomic simulations in the fields of material discovery and property prediction. The review illustrated the application of machine learning models to evaluate the thermodynamic and kinetic properties of Si, LiC, and LiTiO systems. Ziheng Lu [126] discussed use of ML for energy devices including batteries, photovoltaics, and catalysts.

## 1.9 OBJECTIVE

The objectives of this investigation are:

- Development of superior energy storage devices
- Investigation of novel electrode system that work on framework structure to store the electrochemical charge storage based on redox-mediated interaction as well as surface capacitance.
- Synthesis of Oxalate and phosphate-based structure containing transition metal ions such as Ni, Co and Ce by solution based low temperature chemical precipitation methods and investigation as an electrode for pseudocapacitive charge storage in aqueous electrolyte.
- Coupling the developed Electrodes with capacitive carbon electrode to make Hybrid supercapacitor (HSC) type full cell device to obtain real energy and power density of the full cell device.
- Modelling and predicting the performance of HSC type full cell devices, employing various machine learning techniques and developing efficient and predictive surrogate models for different material properties, the screening and selection of new candidate materials for specific applications.

## References

1. Someya, T., Bao, Z., & Malliaras, G. G. (2016). The rise of plastic bioelectronics. *Nature*, 540(7633), 379-385.
2. Chortos, A., Liu, J., & Bao, Z. (2016). Pursuing prosthetic electronic skin. *Nature materials*, 15(9), 937-950.
3. Karimi, F., O'Connor, A. J., Qiao, G. G., & Heath, D. E. (2018). Integrin clustering matters: a review of biomaterials functionalized with multivalent integrin-binding ligands to improve cell adhesion, migration, differentiation, angiogenesis, and biomedical device integration. *Advanced healthcare materials*, 7(12), 1701324.
4. Gong, S., & Cheng, W. (2017). Toward soft skin-like wearable and implantable energy devices. *Advanced Energy Materials*, 7(23), 1700648.
5. Irimia-Vladu, M. (2014). “Green” electronics: biodegradable and biocompatible materials and devices for sustainable future. *Chemical Society Reviews*, 43(2), 588-610.
6. [https://energypedia.info/wiki/Energy\\_for\\_Rural\\_Health\\_Centers](https://energypedia.info/wiki/Energy_for_Rural_Health_Centers)
7. Chatterjee, S., Singh, A., & Kar, S. K. (2022). Service bonds in rural health care in India-Challenges and the way forward. *The Lancet Regional Health-Southeast Asia*, 6.
8. Shastry, V., & Rai, V. (2021). Reduced health services at under-electrified primary healthcare facilities: Evidence from India. *PloS one*, 16(6), e0252705.
9. <https://www.news-medical.net/health/Insight-into-Implantable-Medical-Devices.aspx>
10. Cottenden, A. M., Stocking, B., Jones, N. B., Morrison, S. L., & Rothwell, R. (1981). Biomedical engineering—Priorities for research in external aids. *Journal of Biomedical Engineering*, 3(4), 325-328.
11. Moradkhani, A., Broumandnia, A., & Mirabedini, S. J. (2022). A portable medical device for detecting diseases using Probabilistic Neural Network. *Biomedical Signal Processing and Control*, 71, 103142.
12. Mikołajewska, E., & Mikołajewski, D. (2010). Wheelchair development from the perspective of physical therapists and biomedical engineers. *Advances in Clinical and Experimental Medicine*, 19(6), 771-776.
13. Cao, H., Rao, S., Tang, S. J., Tibbals, H. F., Spechler, S., & Chiao, J. C. (2013). Batteryless implantable dual-sensor capsule for esophageal reflux monitoring. *Gastrointestinal endoscopy*, 77(4), 649-653.
14. Webster, J.G. *Design of Cardiac Pacemakers*; IEEE Press: Piscataway, NJ, USA, 1995.

15. Wilson, B. S., Finley, C. C., Lawson, D. T., Wolford, R. D., Eddington, D. K., & Rabinowitz, W. M. (1991). Better speech recognition with cochlear implants. *Nature*, 352(6332), 236-238.
16. Breit, S., Schulz, J. B., & Benabid, A. L. (2004). Deep brain stimulation. *Cell and tissue research*, 318, 275-288.
17. Ben Amar, A., Kouki, A. B., & Cao, H. (2015). Power approaches for implantable medical devices. *sensors*, 15(11), 28889-28914.
18. Bock, D. C., Marschilok, A. C., Takeuchi, K. J., & Takeuchi, E. S. (2012). Batteries used to power implantable biomedical devices. *Electrochimica acta*, 84, 155-164.
19. Zhai, L., Duan, J., Lin, T., & Shao, H. (2024). Recent Advances in Implantable Batteries: Development and Challenge. *Journal of Alloys and Compounds*, 173551.
20. Chodankar, N. R., Karekar, S. V., Safarkhani, M., Patil, A. M., Shinde, P. A., Ambade, R. B., ... & Alhajri, E. (2024). Revolutionizing implantable technology: biocompatible Supercapacitors as the future of power sources. *Advanced Functional Materials*, 2406819.
21. Hannan, M. A., Mutashar, S., Samad, S. A., & Hussain, A. (2014). Energy harvesting for the implantable biomedical devices: issues and challenges. *Biomedical engineering online*, 13, 1-23.
22. Panda, S., Hajra, S., Mistewicz, K., In-na, P., Sahu, M., Rajaiitha, P. M., & Kim, H. J. (2022). Piezoelectric energy harvesting systems for biomedical applications. *Nano Energy*, 100, 107514.
23. Roy, S., Azad, A. W., Baidya, S., Alam, M. K., & Khan, F. (2022). Powering solutions for biomedical sensors and implants inside the human body: A comprehensive review on energy harvesting units, energy storage, and wireless power transfer techniques. *IEEE Transactions on Power Electronics*, 37(10), 12237-12263.
24. Zheng, Q., Shi, B., Li, Z., & Wang, Z. L. (2017). Recent progress on piezoelectric and triboelectric energy harvesters in biomedical systems. *Advanced Science*, 4(7), 1700029.
25. Scrosati, B. (2011). History of lithium batteries. *Journal of solid state electrochemistry*, 15(7), 1623-1630.
26. Wang, C., Fu, K., Dai, J., Lacey, S. D., Yao, Y., Pastel, G., ... & Hu, L. (2017). Inverted battery design as ion generator for interfacing with biosystems. *Nature communications*, 8(1), 15609.

27. Yin, L., Huang, X., Xu, H., Zhang, Y., Lam, J., Cheng, J., & Rogers, J. A. (2014). Materials, designs, and operational characteristics for fully biodegradable primary batteries. *Adv. Mater*, 26(23), 3879-3884.
28. Baptista, A. C., Martins, J. I., Fortunato, E., Martins, R., Borges, J. P., & Ferreira, I. (2011). Thin and flexible bio-batteries made of electrospun cellulose-based membranes. *Biosensors and Bioelectronics*, 26(5), 2742-2745.
29. Wellman, S. M., Eles, J. R., Ludwig, K. A., Seymour, J. P., Michelson, N. J., McFadden, W. E., ... & Kozai, T. D. (2018). A materials roadmap to functional neural interface design. *Advanced functional materials*, 28(12), 1701269.
30. Ma, Z., Li, S., Wang, H., Cheng, W., Li, Y., Pan, L., & Shi, Y. (2019). Advanced electronic skin devices for healthcare applications. *Journal of Materials Chemistry B*, 7(2), 173-197.
31. James, F. A. (1989). Michael Faraday's first law of electrochemistry: how context develops new knowledge.
32. History of the battery, [https://en.wikipedia.org/wiki/History\\_of\\_the\\_battery](https://en.wikipedia.org/wiki/History_of_the_battery)
33. Das Gupta, S. (1989). *The Search for Portable Electricity: History of High Energy-Density Batteries*.
34. Holmes, C. (2007). The lithium/iodine-polyvinylpyridine pacemaker battery-35 years of successful clinical use. *ECS Transactions*, 6(5), 1.
35. Johnson, C. S. (2007). Development and utility of manganese oxides as cathodes in lithium batteries. *Journal of Power Sources*, 165(2), 559-565.
36. Greatbatch, W., Holmes, C. F., Takeuchi, E. S., & Ebel, S. J. (1996). Lithium/carbon monofluoride (LI/CFx): a new pacemaker battery. *Pacing and clinical electrophysiology*, 19(11), 1836-1840.
37. Takeuchi, E. S., & Piliero, P. (1987). Lithium/silver vanadium oxide batteries with various silver to vanadium ratios. *J. Power Sources;(Switzerland)*, 21(2).
38. Huggins, R. (2008). *Advanced batteries: materials science aspects*. Springer Science & Business Media.
39. Pavlov, D. (2011). *Lead-acid batteries: science and technology*. Elsevier.
40. Tarascon, J. M., & Armand, M. (2001). Issues and challenges facing rechargeable lithium batteries. *nature*, 414(6861), 359-367.
41. Scrosati, B. (1997). *Modern batteries: an introduction to electrochemical power sources*. Arnold.

42. Ruben, S. (1981). Primary Batteries—Sealed Mercurial Cathode Dry Cells. In *Comprehensive Treatise of Electrochemistry: Volume 3: Electrochemical Energy Conversion and Storage* (pp. 233-245). Boston, MA: Springer US.
43. Bullen, R. A., Arnot, T. C., Lakeman, J. B., & Walsh, F. C. (2006). Biofuel cells and their development. *Biosensors and Bioelectronics*, 21(11), 2015-2045.
44. Grove, W. R. (1839). XXIV. On voltaic series and the combination of gases by platinum. *The London, Edinburgh, and Dublin Philosophical Magazine and Journal of Science*, 14(86-87), 127-130.
45. Potter, M. C. (1911). Electrical effects accompanying the decomposition of organic compounds. *Proceedings of the royal society of London. Series b, containing papers of a biological character*, 84(571), 260-276.
46. Cohen, B. (1931). The bacterial culture as an electrical half-cell. *J. Bacteriol*, 21(1), 18-19.
47. Wei, X., & Liu, J. (2008). Power sources and electrical recharging strategies for implantable medical devices. *Frontiers of Energy and Power Engineering in China*, 2, 1-13.
48. May, G. J., Davidson, A., & Monahov, B. (2018). Lead batteries for utility energy storage: A review. *Journal of energy storage*, 15, 145-157.
49. Jeong, H. S., Hong, S. C., & Lee, S. Y. (2010). Effect of microporous structure on thermal shrinkage and electrochemical performance of Al<sub>2</sub>O<sub>3</sub>/poly (vinylidene fluoride-hexafluoropropylene) composite separators for lithium-ion batteries. *Journal of Membrane Science*, 364(1-2), 177-182.
50. Hou, C. L., Wu, J., Zhang, M., Yang, J. M., & Li, J. P. (2004, April). Application of adaptive algorithm of solar cell battery charger. In *2004 IEEE International Conference on Electric Utility Deregulation, Restructuring and Power Technologies. Proceedings* (Vol. 2, pp. 810-813). IEEE.
51. Christensen, J., Albertus, P., Sanchez-Carrera, R. S., Lohmann, T., Kozinsky, B., Liedtke, R., ... & Kojic, A. (2011). A critical review of Li/air batteries. *Journal of the Electrochemical Society*, 159(2), R1.
52. Tang, Y., Yuan, W., Pan, M., Li, Z., Chen, G., & Li, Y. (2010). Experimental investigation of dynamic performance and transient responses of a kW-class PEM fuel cell stack under various load changes. *Applied Energy*, 87(4), 1410-1417.

53. Kollimalla, S. K., Mishra, M. K., & Narasamma, N. L. (2014). Design and analysis of novel control strategy for battery and supercapacitor storage system. *IEEE Transactions on Sustainable Energy*, 5(4), 1137-1144.
54. Dutta, A., Mitra, S., Basak, M., & Banerjee, T. (2023). A comprehensive review on batteries and supercapacitors: Development and challenges since their inception. *Energy Storage*, 5(1), e339.
55. Conway, B. E. (2013). *Electrochemical supercapacitors: scientific fundamentals and technological applications*. Springer Science & Business Media.
56. Arbizzani, C., Mastragostino, M., & Soavi, F. (2001). New trends in electrochemical supercapacitors. *Journal of power sources*, 100(1-2), 164-170.
57. Yan, J., Wang, Q., Wei, T., & Fan, Z. (2014). Recent advances in design and fabrication of electrochemical supercapacitors with high energy densities. *Advanced Energy Materials*, 4(4), 1300816.
58. Häggström, F., & Delsing, J. (2018). Iot energy storage-a forecast. *Energy harvesting and systems*, 5(3-4), 43-51.
59. Wang, G., Zhang, L., & Zhang, J. (2012). A review of electrode materials for electrochemical supercapacitors. *Chemical Society Reviews*, 41(2), 797-828.
60. Sharma, P., & Bhatti, T. S. (2010). A review on electrochemical double-layer capacitors. *Energy conversion and management*, 51(12), 2901-2912.
61. Conway, B. E. (1991). Transition from “supercapacitor” to “battery” behavior in electrochemical energy storage. *Journal of the Electrochemical Society*, 138(6), 1539.
62. Augustyn, V., Simon, P., & Dunn, B. (2014). Pseudocapacitive oxide materials for high-rate electrochemical energy storage. *Energy & Environmental Science*, 7(5), 1597-1614.
63. Dubal, D. P., Ayyad, O., Ruiz, V., & Gomez-Romero, P. (2015). Hybrid energy storage: the merging of battery and supercapacitor chemistries. *Chemical Society Reviews*, 44(7), 1777-1790.
64. Zuo, W., Li, R., Zhou, C., Li, Y., Xia, J., & Liu, J. (2017). Battery-supercapacitor hybrid devices: recent progress and future prospects. *Advanced science*, 4(7), 1600539.
65. Gogotsi, Y., & Penner, R. M. (2018). Energy storage in nanomaterials—capacitive, pseudocapacitive, or battery-like?. *ACS nano*, 12(3), 2081-2083.

66. Wang, J., Polleux, J., Lim, J., & Dunn, B. (2007). Pseudocapacitive contributions to electrochemical energy storage in TiO<sub>2</sub> (anatase) nanoparticles. *The Journal of Physical Chemistry C*, 111(40), 14925-14931.
67. Conway, B. E., Birss, V., & Wojtowicz, J. (1997). The role and utilization of pseudocapacitance for energy storage by supercapacitors. *Journal of power sources*, 66(1-2), 1-14.
68. Lindström, H., Södergren, S., Solbrand, A., Rensmo, H., Hjelm, J., Hagfeldt, A., & Lindquist, S. E. (1997). Li<sup>+</sup> ion insertion in TiO<sub>2</sub> (anatase). 2. Voltammetry on nanoporous films. *The Journal of Physical Chemistry B*, 101(39), 7717-7722.
69. Lv, Q., Li, X., Tian, X., Fu, D. A., Liu, H., Liu, J., ... & Wang, L. (2023). A degradable and biocompatible supercapacitor implant based on functional sericin hydrogel electrode. *Advanced Energy Materials*, 13(16), 2203814.
70. Wang, L., Liu, F., Ning, Y., Bradley, R., Yang, C., Yong, K. T., ... & Wu, W. (2020). Biocompatible mesoporous hollow carbon nanocapsules for high performance supercapacitors. *Scientific reports*, 10(1), 4306.
71. Park, T., Lee, D. Y., Ahn, B. J., Kim, M., Bok, J., Kang, J. S., ... & Jang, Y. (2024). Implantable anti-biofouling biosupercapacitor with high energy performance. *Biosensors and Bioelectronics*, 243, 115757.
72. Liu, S., Wei, L., & Wang, H. (2020). Review on reliability of supercapacitors in energy storage applications. *Applied Energy*, 278, 115436.
73. Liu, C., Li, Q., & Wang, K. (2021). State-of-charge estimation and remaining useful life prediction of supercapacitors. *Renewable and Sustainable Energy Reviews*, 150, 111408.
74. M. Y. Ho, P. S. Khiew, D. Isa, T. K. Tan, W. S. Chiu, and C. H. Chia, "A review of metal oxide composite electrode materials for electrochemical capacitors," *Nano*, 2014, 09, 143-149.
75. Lin, T., Chen, I. W., Liu, F., Yang, C., Bi, H., Xu, F., & Huang, F. (2015). Nitrogen-doped mesoporous carbon of extraordinary capacitance for electrochemical energy storage. *Science*, 350(6267), 1508-1513.
76. Zhou, J., Lian, J., Hou, L., Zhang, J., Gou, H., Xia, M., ... & Gao, F. (2015). Ultrahigh volumetric capacitance and cyclic stability of fluorine and nitrogen co-doped carbon microspheres. *Nature communications*, 6(1), 8503.
77. Dong, X., Jin, H., Wang, R., Zhang, J., Feng, X., Yan, C., ... & Lu, J. (2018). High Volumetric Capacitance, Ultralong Life Supercapacitors Enabled by Waxberry-

- Derived Hierarchical Porous Carbon Materials. *Advanced energy materials*, 8(11), 1702695.
78. Divyashree, A., & Hegde, G. (2015). Activated carbon nanospheres derived from bio-waste materials for supercapacitor applications—a review. *Rsc Advances*, 5(107), 88339-88352.
79. Teo, E. Y. L., Muniandy, L., Ng, E. P., Adam, F., Mohamed, A. R., Jose, R., & Chong, K. F. (2016). High surface area activated carbon from rice husk as a high performance supercapacitor electrode. *Electrochimica Acta*, 192, 110-119.
80. González, J. E. G., & Mirza-Rosca, J. C. (1999). Study of the corrosion behavior of titanium and some of its alloys for biomedical and dental implant applications. *Journal of Electroanalytical Chemistry*, 471(2), 109-115.
81. Gepreel, M. A. H., & Niinomi, M. (2013). Biocompatibility of Ti-alloys for long-term implantation. *Journal of the mechanical behavior of biomedical materials*, 20, 407-415.
82. Trasatti, S. & Buzzanca, G. Ruthenium dioxide: a new interesting electrode material. Solid state structure and electrochemical behaviour. *Electroanalytical chemistry and interfacial electrochemistry*, 1971, 29, 1–5.
83. C. D. Lokhande, D. P. Dubal, and O.-S. Joo, “Metal oxide thin film based supercapacitors,” *Curr. Appl. Phys.*, 2011, 11, 255–270.
84. W. Sugimoto, H. Iwata, K. Yokoshima, Y. Murakami, and Y. Takasu, “Proton and Electron Conductivity in Hydrous Ruthenium Oxides Evaluated by Electrochemical Impedance Spectroscopy: The Origin of Large Capacitance,” *J. Phys. Chem. B*, 2005, 109, 7330–7338.
85. C.-C. Hu, Y.-L. Yang, and T.-C. Lee, “Microwave-Assisted Hydrothermal Synthesis of RuO<sub>2</sub>·xH<sub>2</sub>O–TiO<sub>2</sub> Nanocomposites for High Power Supercapacitors,” *Electrochem. Solid-State Lett.*, 2010, 13, 173-185.
86. T.-F. Hsieh, C.-C. Chuang, W.-J. Chen, J.-H. Huang, W.-T. Chen, and C.-M. Shu, “Hydrous ruthenium dioxide/multi-walled carbon-nanotube/titanium electrodes for supercapacitors,” *Carbon*, 2012, 50, 1740–1747.
87. M. Huang, F. Li, F. Dong, Y. X. Zhang, and L. L. Zhang, “MnO<sub>2</sub> -based nanostructures for high-performance supercapacitors,” *J. Mater. Chem. A*, 2015, 3, 21380–21423.
88. F. Shi, L. Li, X. Wang, C. Gu, and J. Tu, “Metal oxide/hydroxide-based materials for supercapacitors,” *RSC Adv*, 2014, 4, 41910–41921.

89. O. Ghodbane, J.-L. Pascal, and F. Favier, "Microstructural Effects on Charge-Storage Properties in MnO<sub>2</sub> -Based Electrochemical Supercapacitors," *ACS Appl. Mater. Interfaces*, 2009, 1, 1130–1139.
90. J. W. Lee, T. Ahn, J. H. Kim, J. M. Ko, and J.-D. Kim, "Nanosheets based mesoporous NiO microspherical structures via facile and template-free method for high performance supercapacitors," *Electrochimica Acta*, 2011, 56, 4849–4857.
91. S.-I. Kim, J.-S. Lee, H.-J. Ahn, H.-K. Song, and J.-H. Jang, "Facile Route to an Efficient NiO Supercapacitor with a Three-Dimensional Nanonetwork Morphology," *ACS Appl. Mater. Interfaces*, 2013, 5, 1596–1603.
92. K.-C. Liu and M. A. Anderson, "Porous Nickel Oxide/Nickel Films for Electrochemical Capacitors," *J Electrochem Soc*, 1996, 143, 7-9.
93. K.-W. Nam and K.-B. Kim, "A Study of the Preparation of NiO<sub>x</sub> Electrode via Electrochemical Route for Supercapacitor Applications and Their Charge Storage Mechanism," *J. Electrochem. Soc.*, 2002, 149, 346-349.
94. C. Yuan, X. Zhang, L. Su, B. Gao, and L. Shen, "Facile synthesis and self-assembly of hierarchical porous NiO nano/micro spherical superstructures for high performance supercapacitors," *J. Mater. Chem.*, 2009, 19, 5772-5804.
95. Y. Ren and L. Gao, "From Three-Dimensional Flower-Like  $\alpha$ -Ni(OH)<sub>2</sub> Nanostructures to Hierarchical Porous NiO Nanoflowers: Microwave-Assisted Fabrication and Supercapacitor Properties: Rapid Communications of the American Ceramic Society," *J. Am. Ceram. Soc.*, 2010, 93, 3560–3564.
96. M. C. Bernard, P. Bernard, M. Keddad, S. Senyarich, and H. Takenouti, "Characterisation of new nickel hydroxides during the transformation of  $\alpha$  Ni(OH)<sub>2</sub> to  $\beta$  Ni(OH)<sub>2</sub> by ageing," *Electrochimica Acta*; 1996, 41, 91–93.
97. Chen, Z., Peng, Y., Liu, F., Le, Z., Zhu, J., Shen, G., ... & Li, H. (2015). Hierarchical nanostructured WO<sub>3</sub> with biomimetic proton channels and mixed ionic-electronic conductivity for electrochemical energy storage. *Nano letters*, 15(10), 6802-6808.
98. Meng, Q., Cai, K., Chen, Y., & Chen, L. (2017). Research progress on conducting polymer based supercapacitor electrode materials. *Nano Energy*, 36, 268-285.
99. Zhao, Y., Liu, J., Hu, Y., Cheng, H., Hu, C., Jiang, C., ... & Qu, L. (2012). Highly compression-tolerant supercapacitor based on polypyrrole-mediated graphene foam electrodes. *Advanced Materials (Deerfield Beach, Fla.)*, 25(4), 591-595.

100. Zhu, Y. P., Jing, Y., Vasileff, A., Heine, T., & Qiao, S. Z. (2017). 3D synergistically active carbon nanofibers for improved oxygen evolution. *Advanced Energy Materials*, 7(14), 1602928.
101. Luo, J., Zhong, W., Zou, Y., Xiong, C., & Yang, W. (2016). Preparation of morphology-controllable polyaniline and polyaniline/graphene hydrogels for high performance binder-free supercapacitor electrodes. *Journal of Power Sources*, 319, 73-81.
102. Yuan, L., Yao, B., Hu, B., Huo, K., Chen, W., & Zhou, J. (2013). Polypyrrole-coated paper for flexible solid-state energy storage. *Energy & Environmental Science*, 6(2), 470-476.
103. D. P. Dubal, O. Ayyad, V. Ruiz and P. Gomez-Romero, "Hybrid energy storage: the merging of battery and supercapacitor chemistries" *Chem. Soc. Rev.*, 2015, 44, 1777–1790.
104. Wang, L.; Zhang, R.; Jiang, Y.; Tian, H.; Tan, Y.; Zhu, K.; Yu, Z.; Li, W. Interfacial synthesis of micro-cuboid Ni<sub>0.55</sub>Co<sub>0.45</sub>C<sub>2</sub>O<sub>4</sub> solid solution with enhanced electrochemical performance for hybrid supercapacitors. *Nanoscale*, 2019, 11, 13894–13902.
105. Zhao, C.; Jiang, Y.; Liang, S.; Gao, F.; Xie, L.; Chen, L. Twodimensional porous nickel oxalate thin sheets constructed by ultrathin nanosheets as electrode materials for high-performance aqueous supercapacitors. *CrystEngComm.*, 2020, 22, 2953.
106. Cheng, G.; Si, C.; Zhang, J.; Wang, Y.; Yang, W.; Dong, C.; Zhang, Z. Facile fabrication of cobalt oxalate nanostructures with superior specific capacitance and super-long cycling stability. *J. Power Sources.*, 2016, 312, 184–191.
107. Li, X., Xiao, X., Li, Q., Wei, J., Xue, H., & Pang, H. (2018). Metal (M= Co, Ni) phosphate based materials for high-performance supercapacitors. *Inorganic Chemistry Frontiers*, 5(1), 11-28.
108. Jiang, H., Zhao, T., Li, C., & Ma, J. (2011). Hierarchical self-assembly of ultrathin nickel hydroxide nanoflakes for high-performance supercapacitors. *Journal of Materials Chemistry*, 21(11), 3818-3823.
109. Wang, S., Pang, H., Zhao, S., Shao, W., Zhang, N., Zhang, J., ... & Li, S. (2014). NH<sub>4</sub>CoPO<sub>4</sub>·H<sub>2</sub>O microbundles consisting of one-dimensional layered microrods for high performance supercapacitors. *RSC Advances*, 4(1), 340-347.

110. Chen, C., Chen, W., Lu, J., Chu, D., Huo, Z., Peng, Q., & Li, Y. (2009). Transition-metal phosphate colloidal spheres. *Angewandte Chemie*, 121(26), 4910-4913.
111. Botu, V., & Ramprasad, R. (2015). Learning scheme to predict atomic forces and accelerate materials simulations. *Physical Review B*, 92(9), 094306.
112. Lv, C., Zhou, X., Zhong, L., Yan, C., Srinivasan, M., Seh, Z. W., ... & Yan, Q. (2022). Machine learning: an advanced platform for materials development and state prediction in lithium-ion batteries. *Advanced Materials*, 34(25), 2101474.
113. Liu, Y., Wu, J., Yang, G., Zhao, T., & Shi, S. (2019). Predicting the onset temperature ( $T_g$ ) of  $GexSe_{1-x}$  glass transition: a feature selection based two-stage support vector regression method. *Science Bulletin*, 64(16), 1195-1203.
114. Butler, K. T., Davies, D. W., Cartwright, H., Isayev, O., & Walsh, A. (2018). Machine learning for molecular and materials science. *Nature*, 559(7715), 547-555.
115. Zanca, F., Glasby, L. T., Chong, S., Chen, S., Kim, J., Fairen-Jimenez, D., ... & Moghadam, P. Z. (2021). Computational techniques for characterisation of electrically conductive MOFs: quantum calculations and machine learning approaches. *Journal of Materials Chemistry C*, 9(39), 13584-13599.
116. Sun, X., Zheng, J., Gao, Y., Qiu, C., Yan, Y., Yao, Z., ... & Wang, J. (2020). Machine-learning-accelerated screening of hydrogen evolution catalysts in MBenes materials. *Applied Surface Science*, 526, 146522.
117. Xie, Y., Zhang, C., Hu, X., Zhang, C., Kelley, S. P., Atwood, J. L., & Lin, J. (2019). Machine learning assisted synthesis of metal-organic nanocapsules. *Journal of the American Chemical Society*, 142(3), 1475-1481.
118. Ward, L., Agrawal, A., Choudhary, A., & Wolverton, C. (2016). A general-purpose machine learning framework for predicting properties of inorganic materials. *npj Computational Materials*, 2(1), 1-7.
119. Podryabinkin, E. V., Tikhonov, E. V., Shapeev, A. V., & Oganov, A. R. (2019). Accelerating crystal structure prediction by machine-learning interatomic potentials with active learning. *Physical Review B*, 99(6), 064114.
120. Tawfik, S. A., Isayev, O., Stampfl, C., Shapter, J., Winkler, D. A., & Ford, M. J. (2019). Efficient prediction of structural and electronic properties of hybrid 2D materials using complementary DFT and machine learning approaches. *Advanced Theory and Simulations*, 2(1), 1800128.

121. Wu, B., Han, S., Shin, K. G., & Lu, W. (2018). Application of artificial neural networks in design of lithium-ion batteries. *Journal of Power Sources*, 395, 128-136.
122. Schmidt, J., Marques, M. R., Botti, S., & Marques, M. A. (2019). Recent advances and applications of machine learning in solid-state materials science. *npj computational materials*, 5(1), 83.
123. Mater, A. C., & Coote, M. L. (2019). Deep learning in chemistry. *Journal of chemical information and modeling*, 59(6), 2545-2559.
124. Chen, A., Zhang, X., & Zhou, Z. (2020). Machine learning: accelerating materials development for energy storage and conversion. *InfoMat*, 2(3), 553-576.
125. Guan, S. H., Shang, C., & Liu, Z. P. (2021). Structure and dynamics of energy materials from machine learning simulations: A topical review. *Chinese Journal of Chemistry*, 39(11), 3144-3154.
126. Lu, Z. (2021). Computational discovery of energy materials in the era of big data and machine learning: a critical review. *Materials Reports: Energy*, 1(3), 100047.
127. Wang, J., Polleux, J., Lim, J., & Dunn, B. (2007). Pseudocapacitive contributions to electrochemical energy storage in TiO<sub>2</sub> (anatase) nanoparticles. *The Journal of Physical Chemistry C*, 111(40), 14925-14931.
128. Zheng, J. P., Cygan, P. J., & Jow, T. R. (1995). Hydrous ruthenium oxide as an electrode material for electrochemical capacitors. *Journal of the Electrochemical Society*, 142(8), 2699.
129. Soin, N., Roy, S. S., Mitra, S. K., Thundat, T., & McLaughlin, J. A. (2012). Nanocrystalline ruthenium oxide dispersed Few Layered Graphene (FLG) nanoflakes as supercapacitor electrodes. *Journal of Materials Chemistry*, 22(30), 14944-14950.
130. Lee, H. Y., & Goodenough, J. B. (1999). Supercapacitor behavior with KCl electrolyte. *Journal of Solid State Chemistry*, 144(1), 220-223.
131. Devaraj, S., & Munichandraiah, N. (2008). Effect of crystallographic structure of MnO<sub>2</sub> on its electrochemical capacitance properties. *The Journal of Physical Chemistry C*, 112(11), 4406-4417.
132. Liu, K. C., & Anderson, M. A. (1996). Porous nickel oxide/nickel films for electrochemical capacitors. *Journal of the Electrochemical Society*, 143(1), 124.

133. Lee, H. Y., & Goodenough, J. B. (1999). Ideal supercapacitor behavior of amorphous  $V_2O_5 \cdot nH_2O$  in potassium chloride (KCl) aqueous solution. *Journal of Solid State Chemistry*, 148(1), 81-84.
134. Gao, Y., Chen, S., Cao, D., Wang, G., & Yin, J. (2010). Electrochemical capacitance of  $Co_3O_4$  nanowire arrays supported on nickel foam. *Journal of Power Sources*, 195(6), 1757-1760.
135. Xia, X. H., Tu, J. P., Wang, X. L., Gu, C. D., & Zhao, X. B. (2011). Mesoporous  $Co_3O_4$  monolayer hollow-sphere array as electrochemical pseudocapacitor material. *Chemical Communications*, 47(20), 5786-5788.
136. Wang, S. Y., Ho, K. C., Kuo, S. L., & Wu, N. L. (2005). Investigation on capacitance mechanisms of  $Fe_3O_4$  electrochemical capacitors. *Journal of the Electrochemical Society*, 153(1), A75.
137. Liu, X. Y., Zhang, Y. Q., Xia, X. H., Shi, S. J., Lu, Y., Wang, X. L., ... & Tu, J. P. (2013). Self-assembled porous  $NiCo_2O_4$  hetero-structure array for electrochemical capacitor. *Journal of Power Sources*, 239, 157-163.
138. Wilde, P. M., Guther, T. J., Oesten, R., & Garche, J. (1999). Strontium ruthenate perovskite as the active material for supercapacitors. *Journal of Electroanalytical Chemistry*, 461(1-2), 154-160.
139. Hwang, D. K., Kim, S., Lee, J. H., Hwang, I. S., & Kim, I. D. (2011). Phase evolution of perovskite  $LaNiO_3$  nanofibers for supercapacitor application and p-type gas sensing properties of  $LaOCl-NiO$  composite nanofibers. *Journal of Materials Chemistry*, 21(6), 1959-1965.
140. Mefford, J. T., Hardin, W. G., Dai, S., Johnston, K. P., & Stevenson, K. J. (2014). Anion charge storage through oxygen intercalation in  $LaMnO_3$  perovskite pseudocapacitor electrodes. *Nature materials*, 13(7), 726-732.
141. Naiknaware, A. G., Chavan, J. U., Kaldate, S. H., & Yadav, A. A. (2019). Studies on spray deposited Ni doped  $Mn_3O_4$  electrodes for supercapacitor applications. *Journal of Alloys and Compounds*, 774, 787-794.
142. Singha, S. S., Rudra, S., Mondal, S., Pradhan, M., Nayak, A. K., Satpati, B., ... & Singha, A. (2020). Mn incorporated  $MoS_2$  nanoflowers: A high performance electrode material for symmetric supercapacitor. *Electrochimica Acta*, 338, 135815.
143. Chen, J., Zhou, X., Mei, C., Xu, J., Zhou, S., & Wong, C. P. (2016). Pyrite  $FeS_2$  nanobelts as high-performance anode material for aqueous pseudocapacitor. *Electrochimica Acta*, 222, 172-176.

144. Quan, L., Liu, T., Yi, M., Chen, Q., Cai, D., & Zhan, H. (2018). Construction of hierarchical nickel cobalt selenide complex hollow spheres for pseudocapacitors with enhanced performance. *Electrochimica Acta*, *281*, 109-116.
145. Gupta, A., Kushwaha, V., Mondal, R., Singh, A. N., Prakash, R., Mandal, K. D., & Singh, P. (2022). SrFeO<sub>3-δ</sub>: a novel Fe<sup>4+↔</sup> Fe<sup>2+</sup> redox mediated pseudocapacitive electrode in aqueous electrolyte. *Physical Chemistry Chemical Physics*, *24*(18), 11066-11078.
146. N. K. Mishra, A. K. Singh, R. Mondal, P. Singh, NiC<sub>2</sub>O<sub>4</sub>·2H<sub>2</sub>O Nanoflakes: A Novel Redox-mediated Intercalative Pseudocapacitive Electrode for Supercapacitor Applications in Aqueous KOH and Neutral Na<sub>2</sub>SO<sub>4</sub> electrolytes, *ChemistrySelect*, **2022** 7 (21), e202201134.
147. C. Zhao, Y. Jiang, S. Liang, F. Gao, L. Xie, and L. Chen, Two-dimensional porous nickel oxalate thin sheets constructed by ultrathin nanosheets as electrode materials for high-performance aqueous supercapacitors. *CrystEngComm*, **2020**, *22*, 2953.
148. N. K. Mishra, R. Mondal and P. Singh, Synthesis, characterizations and electrochemical performances of anhydrous CoC<sub>2</sub>O<sub>4</sub> nanorods for pseudocapacitive energy storage applications, *RSC Adv.*, **2021**, *11*, 33926-33937.
149. T. Liu, G. Shao, M. Ji, and Z. Ma Composites of olive-like manganese oxalate on graphene sheets for supercapacitor electrodes *Ionics*, **2014**, *20* 145–149.
150. W. Liu, Y. Song, H. Wang, H.-F. Wang and L. F. Yan, 3D macro-micro-mesoporous FeC<sub>2</sub>O<sub>4</sub>/ graphene hydrogel electrode for high performance 2.5 V aqueous asymmetric supercapacitors, *Chinese J. Chem. Phys.*, 2018, *31* 707–716.
151. N. K. Mishra, R. Mondal, T. Maiyalagan, and P. Singh, Synthesis, Characterizations, and Electrochemical Performances of Highly Porous, Anhydrous Co<sub>0.5</sub>Ni<sub>0.5</sub>C<sub>2</sub>O<sub>4</sub> for Pseudocapacitive Energy Storage Applications, *ACS Omega* **2022**, *7*, 2, 1975–1987.
152. R. Mondal, K. G. Nigam, N. K. Mishra, A. Gupta, and P. Singh, Intercalative pseudocapacitive anhydrous NiC<sub>2</sub>O<sub>4</sub> quantum dot electrode for the fabrication of supercapacitor using aqueous KOH and neutral Na<sub>2</sub>SO<sub>4</sub> electrolyte, *Journal of Energy Storage*, **2023**, *60*, 106549.
153. Cheng, G., Si, C., Zhang, J., Wang, Y., Yang, W., Dong, C., & Zhang, Z. (2016). Facile fabrication of cobalt oxalate nanostructures with superior specific capacitance and super-long cycling stability. *Journal of Power Sources*, *312*, 184-191.